NAVAL POSTGRADUATE SCHOOL

MONTEREY, CALIFORNIA

THESIS

EFFECTS OF METOC FACTORS ON EW SYSTEMS AGAINST LOW DETECTABLE TARGETS IN A TROPICAL LITTORAL ENVIRONMENT

by

Jorge V. Vazquez Zarate

September 2004

Thesis Advisor:	Kenneth L. Davidson
Second Reader:	David C. Jenn

Approved for public release; distribution is unlimited

THIS PAGE INTENTIONALLY LEFT BLANK

REPORT DOCUMENTATION PAGE			Form Approved OMB No. 0704-0188
Public reporting burden for this collection of information is estimated to average 1 hour per response, including the time for reviewing instruction, searching existing data sources, gathering and maintaining the data needed, and completing and reviewing the collection of information. Send comments regarding this burden estimate or any other aspect of this collection of information, including suggestions for reducing this burden, to Washington headquarters Services, Directorate for Information Operations and Reports, 1215 Jefferson Davis Highway, Suite 1204, Arlington, VA 22202-4302, and to the Office of Management and Budget, Paperwork Reduction Project (0704-0188) Washington DC 20503.			
1. AGENCY USE ONLY	**2. REPORT DATE** September 2004	**3. REPORT TYPE AND DATES COVERED** Master's Thesis	
4. TITLE AND SUBTITLE: Effects of METOC Factors on EW Systems Against Low Detectable Targets in a Tropical Littoral Environment			**5. FUNDING NUMBERS**
6. AUTHOR(S) Vazquez Zarate, Jorge V.			
7. PERFORMING ORGANIZATION NAME(S) AND ADDRESS(ES) Naval Postgraduate School Monterey, CA 93943-5000			**8. PERFORMING ORGANIZATION REPORT NUMBER**
9. SPONSORING /MONITORING AGENCY NAME(S) AND ADDRESS(ES) N/A			**10. SPONSORING/MONITORING AGENCY REPORT NUMBER**
11. SUPPLEMENTARY NOTES The views expressed in this thesis are those of the author and do not reflect the official policy or position of the Department of Defense or the U.S. Government.			
12a. DISTRIBUTION / AVAILABILITY STATEMENT Approved for public release; distribution is unlimited			**12b. DISTRIBUTION CODE**

13. ABSTRACT (maximum 200 words)

In Littoral Warfare (LW), naval operations face a whole new range of missions and types of threats. In such situations, Electronic Warfare (EW) systems are extremely important, yet constantly challenged to perform faster and more accurate detection and recognition of potential threats. However, meteorological and oceanographic (METOC) factors can severely modify the effectiveness of EW systems, particularly against low detectable targets in warm waters.

Therefore, this thesis analyzes the effects of tropical littoral environments in the expected performance of generic RF and IR systems when used under these scenarios. It analyzes the outputs of propagation models included in the software suites AREPS and TAWS when using actual data from different sources in the Yucatan Channel.

The results of this study demonstrated how radically the environmental conditions can change, clearly modifying the efficiency of surveillance and detection systems in shipborne platforms. Further, several issues related to the need of valuable data and additional research are addressed, while providing useful insights to operational commanders and decision makers for the use of EW systems and available Tactical Decision Aids (TDAs) at the typical scenarios of Littoral Warfare in tropical waters.

14. SUBJECT TERMS Littoral Warfare, Tactical Decision Aids, Radar, IR, TAWS, AREPS, Refractivity, Propagation, Attenuation, ESM, EW, Probability of Detection, Performance.			**15. NUMBER OF PAGES** 101 / **16. PRICE CODE**
17. SECURITY CLASSIFICATION OF REPORT Unclassified	**18. SECURITY CLASSIFICATION OF THIS PAGE** Unclassified	**19. SECURITY CLASSIFICATION OF ABSTRACT** Unclassified	**20. LIMITATION OF ABSTRACT** UL

NSN 7540-01-280-5500 Standard Form 298 (Rev. 2-89)
Prescribed by ANSI Std. 239-18

THIS PAGE INTENTIONALLY LEFT BLANK

Approved for public release; distribution is unlimited

EFFECTS OF METOC FACTORS ON EW SYSTEMS AGAINST LOW DETECTABLE TARGETS IN A TROPICAL LITTORAL ENVIRONMENT

Jorge V. Vazquez Zarate
Lieutenant Commander, Mexican Navy
B.S., Mexican Naval School, 1990

Submitted in partial fulfillment of the
requirements for the degree of

MASTER OF SCIENCE IN SYSTEMS ENGINEERING MANAGEMENT

from the

NAVAL POSTGRADUATE SCHOOL
September 2004

Author: Jorge V. Vazquez Zarate

Approved by: Kenneth L. Davidson
Thesis Advisor

David C. Jenn
Second Reader

Dan C. Boger
Chairman, Department of Information Sciences

THIS PAGE INTENTIONALLY LEFT BLANK

ABSTRACT

In Littoral Warfare (LW), naval operations face a whole new range of missions and types of threats. In such situations, Electronic Warfare (EW) systems are extremely important, yet constantly challenged to perform faster and more accurate detection and recognition of potential threats. However, meteorological and oceanographic (METOC) factors can severely modify the effectiveness of EW systems, particularly against low detectable targets in warm waters.

Therefore, this thesis analyzes the effects of tropical littoral environments in the expected performance of generic RF and IR systems when used under these scenarios. It analyzes the outputs of propagation models included in the software suites AREPS and TAWS when using actual data from different sources in the Yucatan Channel.

The results of this study demonstrated how radically the environmental conditions can change, clearly modifying the efficiency of surveillance and detection systems in shipborne platforms. Further, several issues related to the need of valuable data and additional research are addressed, while providing useful insights to operational commanders and decision makers for the use of EW systems and available Tactical Decision Aids (TDAs) at the typical LW scenarios in tropical waters.

THIS PAGE INTENTIONALLY LEFT BLANK

TABLE OF CONTENTS

LIST OF FIGURES

LIST OF TABLES

THIS PAGE INTENTIONALLY LEFT BLANK

I. INTRODUCTION

A. THE CONCEPT OF LITTORAL WARFARE

In the last decade, naval operations have significantly shifted from high seas (blue-ocean) engagements to what is known as Littoral Warfare (LW), which has been growing in both strategic and tactical significance, as well as complexity. Littoral regions have been defined as the seas and oceans such that they are directly under control of and vulnerable to the striking power of sea-based forces (Ellington, 1995). LW, therefore, relates to the dominance of the oceans and seas adjacent to the coast from which maritime countries obtain most of their power and resources. However, this concept also implies that the operating naval forces must face a large variety of challenges such as tides, reefs, shallow waters, and mines while dealing with confined seas and air space, congested by both military and civilian traffic.

Naval operations are now responding to new types of warfare, such as asymmetric warfare and the war against terrorism. In these modalities, the enemy is very likely to use small cheap weapons with unconventional tactics against large objectives, trying to cause major impacts, not only in the fighting elements themselves, but in the population and the surrounding environment as well. Moreover, navies are increasingly involved in "Military Operations Other than War" (MOOTW), which frequently include maritime interdiction and traffic control, search and rescue, and law enforcement operations, for example, against drug trafficking and piracy.

To remain current with the complexity of such scenarios, the use of Electronic Warfare (EW) systems is extremely important. In LW, the rapid and accurate identification of potential threats and targets can represent the difference between success and failure in the achievement of the mission, and even the survivability of the fighting platform itself; hence, the relevancy of high performance modern EW systems. Meteorological and oceanographic (METOC) factors can severely modify their performance and effectiveness, particularly in tropical regions, which usually imply high water vapor content in the air above the surface, and high probability of layering with anomalous electromagnetic propagation conditions.

METOC characteristics of tropical littorals have been widely studied, but mostly for purposes other than their impact on littoral naval warfare. There are several studies regarding the factors involved in the anomalies of propagation of Electromagnetic (EM) and Infrared (IR) waves through the atmosphere. However, they do not focus on the performance of both radar and IR systems under the encountered conditions in tropical littoral environments, where often METOC data sources are not sufficient and/or adequate enough. The reliable evaluation of such performances does not seem to have been thoroughly assessed, and needs to be resolved for the proper employment and efficiency of these systems, especially when they are expected to perform against small targets with low detectability.

There are several computer-based effects tools known as Tactical Decision Aids (TDAs), which include models to analyze the expected propagation conditions by using the available data of atmospheric variables. They are capable of providing very helpful and timely guidance about such conditions. Yet their use in tropical littoral environments demands more careful evaluations of their performance, which has not been thoroughly done. This can be critical for highly valuable assets, and thus, will be the main thrust for this study, which will focus on the issues of anomalous propagation patterns and their impact for operational purposes.

B. ORGANIZATION OF THIS WORK

This study will evaluate the effects of abnormal atmospheric conditions on the performance of generic EW systems, based on the use of Tactical Decision Aids (TDAs) and the existing sources of METOC data in a typical tropical littoral scenario. Therefore, some essentials in EW systems and their relationship with LW issues will be discussed in Chapter II. To maintain the general applicability of this work, it will be based upon common radar and IR devices, with generic characteristics and technical specifications for commercially available off-the-shelf (COTS) equipment, resembling actual systems currently in use.

Chapter III describes the theoretical background of the main atmospheric factors involved in the performance of EW systems, as well as the propagation TDAs used for the evaluation of such factors in this study, AREPS (Advanced Refractive Environment Prediction System) and TAWS (Tactical Acquisition of Weapons Systems).

Chapter IV frames this work in the northwestern Caribbean Sea, namely in the Yucatan Channel, defining three specific case studies according to the available METOC data sets, the climatology for this region, and the expected existence of anomalies in EM and IR propagation year round.

Case studies will be analyzed in detail in Chapter V, based upon the outputs from AREPS using climatological data sets, and then compared with their outputs when actual data from alternative sources is used. Next, Chapter VI will discuss some issues for the employment of IR devices in shorter ranges, where they can actually interact with Radar and ESM systems, and the expected effects of the environment in the overall performance.

Finally, Chapter VII summarizes the results and conclusions of this study that may provide further insights and guidelines to assist operational commanders and mission planners in their decision making processes. It also discusses the achievable benefit of allocating additional resources and better procedures to provide more accurate local data, including alternative sources for LW purposes. Some proposals for further research to support the improvement of effectiveness in LW missions will also be addressed.

THIS PAGE INTENTIONALLY LEFT BLANK

II. EW SYSTEMS IN LW

Increasingly restrictive rules of engagement in contemporary naval operations are reducing the time frames for making critical decisions. The use of automated systems for the detection of moving targets, stabilization of platforms, and targeting functions, has allowed shortened response times, as well as interaction with other ship systems for fire control and monitoring. However, this also requires more and better information, with much faster processing for feedback and control purposes in near real-time.

One approach to provide the required data has been the integration of complementary sensors. The combination of different radars, Electronic Support Measures (ESM), Electro-Optical/Infrared (EO/IR) sensors, and sometimes Light Detection and Ranging (Lidar) can allow the exploitation of spatial and frequency diversity, as well as overcoming each sensor's weaknesses while enhancing their respective strengths. Therefore, it is always important to maintain a clear perception of the achievable performances for each system.

A. ES SYSTEMS

Traditionally, Electronic Support (ES) and ES Measures (ESM) were aimed to reconstruct the EM scenario in the environment (known as Electronic Order of Battle, or EOB) in almost real time for self defense purposes, by discovering the presence of enemy platforms with passive surveillance of a wide area. According to current doctrines, Electronic Warfare Support (ES) is now a much broader concept, involving all sorts of tasks under the direct control of an operational commander to search for, intercept, identify, and locate sources of intentional and unintentional radiated EM energy for the purpose of immediate threat recognition, targeting, and the supply of information that enables the implementation of proper Electronic Attack (EA) and Electronic Protection (EP) actions, planning, and conduct of future operations (JCS Joint Pub. 3-51).

ESMs can provide passive intercept, analysis and direction finding capability against RF signals of interest, as well as crucial information for targeting over-the-horizon weapon systems at long range, typically out to approximately 70-90 km.

Such a RF scenario may be truly complex, thus, ESM systems can be much more than a simple Radar Warning Receiver (RWR). They may be equipped with many auxiliary circuits, sometimes even forming a complete surveillance network. Typical naval ESM systems usually work between 0.5-18 GHz, with slant (45°) or circular polarizations, and sensitivities from about -50 to -65 dBm (Neri, 1991, p. 349).

However, ESMs have some drawbacks that may degrade the essential high performance of the combat system. They rely only on the emissions from active sources, and may not be able to detect emissions from Low Probability of Intercept (LPI) radars. Conventional ESMs can also be easily degraded because of reflected signals and multipath effects, the increased number and complexity of operations in congested littorals, and more sophisticated radar techniques (such as agility, jittering, modulation, compression, multimode and rapid mode changes).

B. RADAR SYSTEMS

Radars are essential components of the ship's fire control and self defense systems because of their 3-D detection and tracking capabilities in almost any weather against threats approaching from both air and sea. Most countries use powerful long-range radars in their defense systems for early warning purposes, but for LW, short to medium range radars with higher resolution are preferred in order to cope with "hard to detect" targets such as helicopters, small fast boats, and sea skimming missiles.

All radar signals can be reflected from any surface, but there will be an inherent phase shift. Additionally, differences in length between direct and reflected paths will result in an additional phase shift. The resultant phase differences will produce either a constructive or destructive interference, so the overall propagation will be in a lobing pattern, as shown in Figure 1.

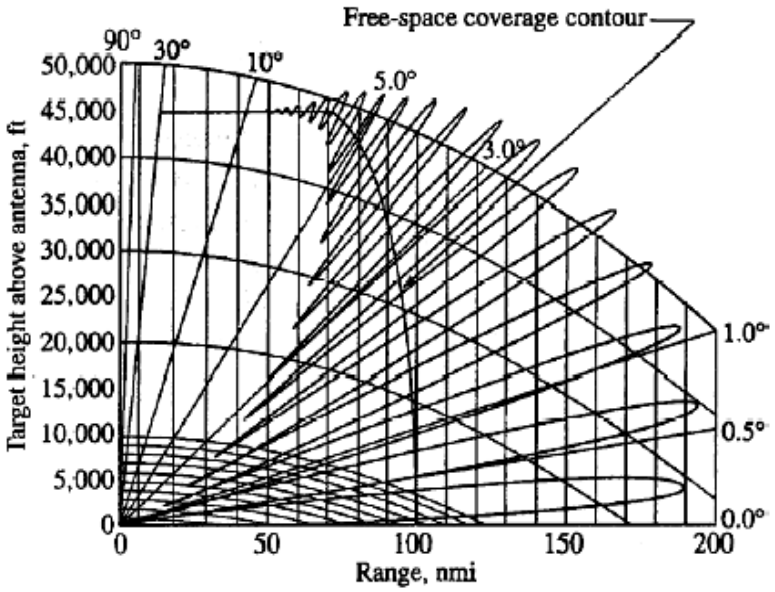

Figure 1. Lobing effect in antenna radiation pattern (From Skolnik, 2001, p. 491)

This pattern can be severely modified by many different factors such as terrain features and atmospheric refraction. They are very hard to account for, but their effects may be computed by rays tracing techniques and refractivity models, one of whose outcome can be the expected spatial distribution of the signal intensity levels.

The new Multifunction Radars (MFRs) are single radar suites of high performance phased arrays, such as Lockheed Martin's S (E/F) band fixed array AN/SPY-1 family used in the Aegis combat systems. Those MFRs are designed to detect and track anti-shipping missile threats, continuous wave target illumination, missile mid-course guidance, and terminal homing for weapons such as RIM-7P Sparrow and the Evolved SeaSparrow Missile (ESSM). Further improvements have been achieved with Active Phased Arrays radars, such as the Alenia Marconi S (E/F) band SAMPSON, and the X (I/J) band APAR from Thales (Janssen, 2002). They can provide 360º coverage in azimuth and up to 70º in elevation, with maximum ranges varying from 32 km (surface search) to 150 km (air-target/back-up volume search), and able to track more than 150 surface targets or more than 200 air targets.

The problems with the MFR technology are the high costs, and their size restricts them to large ships. As a consequence, there have been significant efforts to develop lighter versions with similar technology and architecture. They can now be integrated

into a smaller vessel's superstructure or elevated rotating plate arrays, enabling them for multi-engagement scenarios, so they may be the core of surface/anti-air self defense and limited local area defense for more effective littoral ships.

However, radars may have several inherent drawbacks for LW. They are all active systems, and in the littorals it is often undesirable to transmit any signal that might be exploited by enemy systems or interfere with several other RF devices near the coast. Additionally, many existing naval radars were designed for "blue water" operations, and may not be necessarily able to cope with low detectable targets; particularly when operating under conditions of severe clutter, jamming and accidental interference, main beam multipath effects, and imprecise estimation of target characteristics, which are usual in such an environment.

Another important issue is due to atmospheric refraction. For example, weapon control radars must effectively keep track of the designated targets, direct that weapon to an intercept, and assess the effectiveness of the engagement (Battle Damage Assessment). Although all these functions rely on the high accuracy of the radar's range and direction measurements, the anomalies of EM propagation in the atmospheric conditions normally encountered in tropical littorals can be the cause of severe changes in the range of detection capabilities and elevation angle tracking distortions.

C. EO/IR SENSORS

The limitations of radar systems in the cluttered littoral environment, and technological advances recent years in Electro-optical (EO) sensors, such as thermal imagers exploiting the infrared (IR) spectrum, led to the use of EO Tracking and Fire Control Systems (EOTFCS). They offer passive detection and positive identification at ranges of 15-20 km, with high line-of-sight target pointing accuracy, high quality visual imagery to enable positive target identification, tracking for small and medium caliber weapons control, and low susceptibility to jamming and other countermeasures.

Performance-wise, EO/IR sensors have some advantages over radar-based systems. They are not hampered by mirror effects or by lobing at low elevations, and perform well against slow-moving low signature targets in cluttered environments. They achieve higher resolution and update rates, and are harder to counter since radar

countermeasures do not affect them, while flares and smoke have only limited effect on their performance. Furthermore, anti-ship missiles cannot avoid aerodynamic heating, and consequently are very visible to IR sensors regardless of their stealthy design.

IR sensors have proven to be very useful for threat alert and weapon/sensor cueing applications. Currently, several Infrared Search and Track (IRST) systems are designed for advanced surveillance and tracking against all types of aerial and surface targets in cold or warm waters. This capability is indispensable for the stealthy operation of the ship when the EMCON conditions do not allow the use of radars. They can normally include dual-band (3-5 and 8-12 μm) high resolution third generation thermal imagers, CCD daylight TV cameras, video trackers, and eye-safe laser range-finders (ESLRFs). Some examples are the VAMPIR MB from SAGEM/EADS, SIRIUS from Thales, and MSP500 from STN Atlas Elektronik (Scott, 2003).

The U.S. Navy is improving the Boeing Thermal Imaging Sensor System (TISS), the SeaFLIR AN/KAX systems, and developing a new IRST system on major surface combatants, featuring a 3-5 μm thermal imager with a 512 x 484 element InSb detector, a dual field-of-view CCD TV and a Class 1 eye-safe laser rangefinder, all mounted in a spherical director assembly with reduced jittering of 15 mrad (Janssen, 2003).

EOTFCS are increasingly used onboard many major surface warships as an adjunct or alternative gun fire control within a wider combat system; but they have also become a low cost weapon control system option for smaller warships such as mine countermeasures vessels, offshore patrol vessels, and patrol crafts. Besides their use for detection and tracking of low altitude air and surface targets, they allow the crew to identify any contacts visually in the area at night and in reduced visibility, and even the possibility of recording events for use as legal evidence, thus becoming valuable multipurpose tools to maintain high-quality situational awareness, navigation support, moored mine detection, covert surveillance and protection against asymmetric threats, among others.

There is a wide variety of low cost EO/IR surveillance and/or fire control systems available on the market, such as the Radamec EOS for small patrol boats. It normally has a 3-5 μm thermal imager, and may include a compact TV camera, optional laser range-finder, and/or low light level TV (LLLTV). Other examples are the MEDUSA from Alenia Marconi, NAJIR from EADS, the RADAMEC 2500, SAFIRE from FLIR Systems, and IRSCAN and MIRADOR from Thales.

However, their normal range performances are rather small. For example, the EOS typical performance would be over 20 km to detect and classify a 25 x 25 m merchant vessel, 13.8 km to detect a 6 x 6 m fishing boat and 8.3 km to classify it, and nearly 1,000 m to detect and classify a person. This is a very important consideration when defining a target for analysis, and when conducting comparisons of performance for these systems.

D. INTEGRATION OF MULTIPLE SENSORS

A new trend in modern warfare is the use of surface and anti-air warfare suites, combining volume search and target designation radars with fire control tracking and illumination (I/J-band) radars, generally supported by coaxially-mounted EO adjuncts and laser range-finders. Some examples of target designation radars widely used are the EADS TRS-3D, the Ericsson Sea Giraffe, the Thales MRR, Sea Tiger and SMART-S. Typical tracking and illumination radars can provide fire control of medium caliber guns as well as semi-active homing of radar guided missiles, such as the IAI Elta EL/M-2221, and the SaabTech Systems CEROS 200 (Janssen, *Op. Cit*., 2003).

Sensor and processing improvements in the latest generation of EOTFCS allowed the development of lightweight low RCS (stealthy) directors, intelligent digital trackers, and rationalized electronics packages. It is now common to integrate third generation mid-waveband (3-5 μm) thermal imagers with Mercury Cadmium Telluride (MCT) detectors in EO directors as part of unified combat systems controlled through a standard multifunction console.

IRST systems are also commonly used as a complement to the MFRs, with superior performance against low level close threats. They improve the tracking performance, with the radar providing the accurate range, and IRST providing spatial

resolution with better recognition and identification of targets, which may gain vital extra seconds for hard-kill weapons or soft-kill countermeasures to be deployed effectively. Nevertheless, limitations inherent for each system will still play an important role, so their combined effects should be carefully addressed.

Standard conditions are seldom found in real engagement scenarios, thus the assumptions and compensations made are frequently inaccurate. Despite the technical improvements of the EW systems employed, they will always be subject to the atmospheric propagation effects, so proper corrections must be made for the specific environment where each system is expected to perform.

For example, atmospheric subrefractive conditions can reduce the achievable ranges for both ESM and radar systems, just as superrefractive conditions can significantly increase them as well. Normally, the expected detection ranges for radars are shorter than those for ESMs in similar frequency bands because they perform under a "two-way" propagation basis; but when anomalous refractivity happens, it affects any emission source as well, so the ESMs performance would be inadvertently modified due to their passive nature.

Another example may be when an EMCON condition of radar silence makes the ship depend solely on the IRST component, or when expected threats exceed the IRST capabilities (such as out of line of sight, maximum range, or against a cluttered background with limited thermal contrast), relying then on radar effectiveness only. Therefore, it is extremely important to be aware of when and where such limitations may significantly modify the system performance.

E. SOME CONSIDERATIONS ABOUT ANALYSIS OF PERFORMANCES

Radars and ESMs have been considered to perform fairly well in almost any weather conditions when the right settings and adjustments are made. However, as explained, anomalous refraction can severely modify their propagation paths. This effect is hard to detect and even harder to measure so their performance can be seriously degraded.

In the case of thermal imaging devices, they detect IR waves emanating from the targets, so their performance is more affected by attenuation because of absorption and

scattering of the IR energy rather than refraction, as in the case of radars. This is mainly due to the atmosphere components such as water vapor and oxygen molecules, as well as aerosols suspended in the atmosphere.

ES and IR systems are generally described by different performance parameters, sometimes technically complex and difficult to evaluate. Range, spectral response, resolution and sensitivity are some examples of usual MOPs. Another common MOP may be the achievable probability of detection, which is a primary function for both, assuming specific operational conditions such as range and target characteristics.

There are several ways to account for radar performance evaluations. For example, the radar range equation has several versions (Skolnik, 2001); one of them is:

$$R = \left[\frac{N_i P_T n G_T G_R \sigma \lambda^2}{(4\pi)^3 kTBF\left(S/N\right)_{P_{dfa}} L} F_{pt}^2 \right]^{1/4} \tag{2.1}$$

In this equation, the achieved range is expressed as a function of the transmitted power P_T, the number of pulses integrated N_i, the gain of the antenna for transmission G_T and for reception G_R, the radar cross section of the target σ, and the wavelength λ. The denominator accounts for the noise of the system by using the Boltzmann's constant k, the absolute temperature T, bandwidth B and noise factor F. It also includes the signal-to-noise ratio S/N required to achieve certain probability of detection with a given false alarm rate P_{dfa}, and all the losses of the system grouped by the term L, excluding the atmospheric effects.

Radar is less affected by atmosphere than are optical and IR sensors, unless they use higher microwave and millimeter frequencies. Any energy traveling through the atmosphere suffers from atmospheric attenuation, but for lower frequencies (below 10 GHz), the attenuation is reasonably predictable. Although it is not usually strong enough to be a factor, it is normally accounted for by the propagation factor (F_{pt} in the range equation), generally assuming an exponential behavior. For higher frequencies in the millimeter wave range, the attenuation increases and becomes more dependent upon absorbing characteristics of H_2O and O_2, as shown in Figure 2.

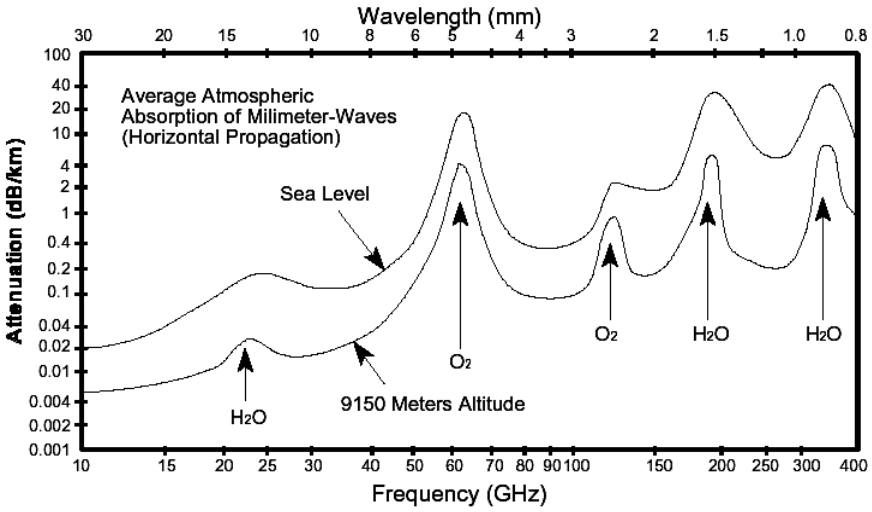

Figure 2. Atmospheric attenuation (From NAVAIR, 1997)

Precipitation backscatter can become important when the wavelength is similar or smaller than the raindrop diameter. Echoes from precipitation can mask a target for frequencies above the X (I/J, 10 GHz) band. For this reason, most of the tracking radars work in this band, achieving the best resolution and accuracy performance with the least degraded propagation.

A major problem with the radar range equation is that lobing and refraction effects are hard to include in such expressions, since the propagation factor does not account for it. There are actually some tools, such as the Advanced Refractive Environmental Prediction Software (AREPS), that allow analysis of performances for both ES and Radar systems, since they work basically in the same RF bands and the atmospheric effects mentioned above are related to the EM frequencies, or equivalently the corresponding wavelengths, rather than any other characteristic of the employed signals.

For the purposes of this study, some "generic" radars will be analyzed. The parameters utilized resemble those of three different commercially available off-the-shelf systems, according to Table 1:

	L (D) Band	S (F) Band	X (I/J) Band
P_T (KW)	120.0	145.0	1000.0
f (MHz)	1250.0	3500.0	10000.0
Pulsewidth (msec)	7.0	0.1	2.0
PRF (Hz)	3400.0	2400.0	800.0
G_T (dB)	23.0	35.0	40.0
G_R(dB)	23.0	35.0	40.0
Noise Factor (dB)	4.0	5.0	5.0
G side lobes (dB)	-57.0	-10.0	-10.0
L (dB)	5.00	3.00	3.00
Doppler bandwidth (Hz)	3400.00	200.00	200.00
Freqw. Agility bandwidth (MHz)	50.00	400.00	200.00
Azimuth beamwidth (deg)	6.00	2.00	3.00
Azimuth scan rate (deg/sec)	90.00	60.00	60.00
P_d	0.5	0.5	0.5
False alarm rate	1e-006	1e-008	1e-008
Maximum detection range (nmi)	60.65	55.94	139.02

Table 1. Basic parameters of three generic radars.

Similarly, in the range equation for IR devices, the main problem is accounting for atmospheric transmittance. More complex models, such as LOWTRAN, have been included in certain TDAs, and they will be discussed in more detail in Chapter VI.

III. METOC FACTORS THAT INFLUENCE THE EM PROPAGATION

In free space (a vacuum), electromagnetic waves propagate in straight paths, but in the atmosphere, they have different behaviors. Radar frequencies, ranging from VHF to the MM waveband (30 MHz to 300 GHz) according to IEEE (Skolnik, 2001, p. 12), are considered to propagate as space waves (either direct or reflected), mostly affected by attenuation, scattering, and refraction.

Their primary path is direct, so to meet the system's objectives, both the target and transmitter must be within the radio horizon, which can be approximately 1/3 larger than the visual horizon, due to normal refraction effects. This rule of thumb will also depend on the height of both the transmitting and the receiving elements, based on the formula

$$d = \sqrt{2h_t + 2h_r} \tag{3.1}$$

where d is the maximum transmitter-receiver distance in nautical miles, while h_t and h_r are the heights in feet of the transmitting and the receiving antennas, respectively.

A. REFRACTION

Vertical spatial variations in the atmosphere produce different speeds of propagation along the EM wave front. When this happens, the wave front is refracted. Of course, the ray path, which is normal to the wave front, is modified. This could lead to over-the-horizon ranges or an apparent position of a detected target being different than its actual position.

EM waves can travel faster in lower indexes of refraction. The ratio of the propagation speed in free space c to the propagation speed in the actual medium n is called index of refraction n:

$$n = c / v \tag{3.2}$$

The typical values of the index of refraction are about 1.000315 for the standard atmosphere at sea level; this value indicates a speed very near to that in free space.

However, the influence along a wave front over a long path yields significant differences for different atmosphere conditions. Further, to have a variable that reflects that difference more readily, a refractivity N is defined as

$$N = (n - 1)\, x\, 10^6 \tag{3.3}$$

The index n, or refractivity N, is expected to decrease with height. At a boundary, the wave path will always be refracted towards the medium with higher n, according to Snell's Law:

$$n_1 \cdot \sin f_1 = n_2 \cdot \sin f_2 \tag{3.4}$$

When the incidence angle f_1 is large enough, and depending also on the n values, the angle f_2 can approach 90°, Further increases in f_1 would result in a complete reflection called the *critical angle*. This is important for surface surveillance, because the desired propagation ray paths are almost parallel to potential layers in the lower atmosphere. Although strict reflection does not occur in the atmosphere, refraction can be severe as to completely bend the wave back to the surface. Thus, the refraction can be viewed as a virtual reflection.

Snell's law also predicts that the radius r of the ray path is determined by the index of refraction gradient as $r = -1/(dn/dz)$, where the negative value is used to have a positive radius for a ray, and bends downward from the geometric $dn/dz = 0$ (a flat surface with infinite radius).

Surface observations can provide good insights into the effects of refractivity, but when refractivity profiles are complex, such as in ducting conditions, errors can be significant. For example, the geometric height z_1 of an object above the surface at a distance d, using an Earth's radius r_e can be approximated by the expression $z = d^2/2r_e$.

The apparent height z of that target for a refracted path (geometric height z_1, minus the refraction effects z_2, as shown in Figure 3), can be determined by using an equivalent radius of curvature $r = -10^6/(dN/dz)$.

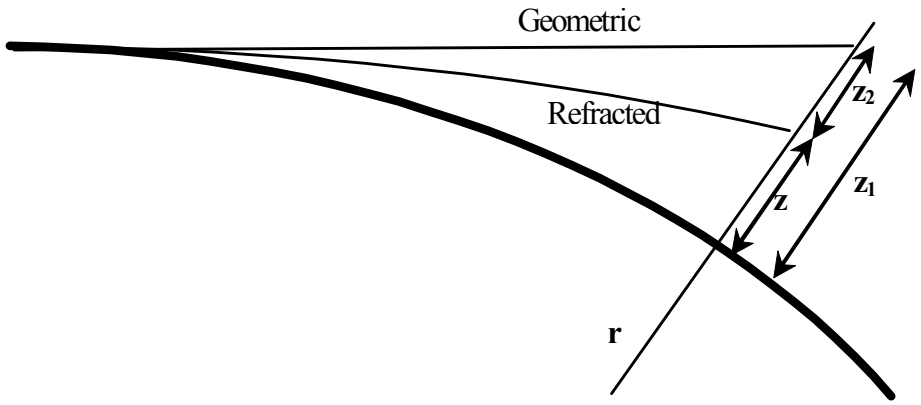

Figure 3. Refraction induced errors in elevation angles

In standard conditions (when $dN/dz \approx$ -40/km) that radius is about 4/3 of the real, so the expression to determine z becomes (from Davidson, 2003, p. 3-13):

$$z = z_1 - z_2 = \frac{d^2}{2}\left(\frac{1}{r_e} + 10^{-6}\frac{dN}{dz}\right) = \frac{d^2}{2}\left(\frac{3}{4r_e}\right) \tag{3.5}$$

As a consequence, it is clear that any radar can produce wrong positions if no accurate corrections for atmospheric refraction are made, or they are based only on standard values; depending on the method used to compute the heights of observed targets, the differences between those and the real positions for low elevation angles might be of hundreds of feet.

B. DUCTING EFFECTS

When an atmospheric layer shows significant anomalies in the expected n gradient, such as thermal inversions and abrupt humidity changes, and the incident angle from the rays is close to the critical angle, it can act as a waveguide for the propagating radio waves (VHF or higher), and may trap them in a duct parallel to earth's surface. To identify trapping conditions, a modified index of refraction M is applied, accounting for an index of refraction gradient that would lead to a ray with radius equal to the earth's radius, being

$$M(z) = N(z) + (z / r_e)\cdot 10^6 = N(z) + 0.157\ Z \tag{3.6}$$

where $r_e \approx$ 6,400 km, and Z is the height about the surface in meters.

Positive N gradients will produce refraction upward (subrefraction), and negative gradients, downward. For practical purposes, M units are more useful because it is easier to determine the occurrence of ducts. When $dM/dz = 0$, the ray paths will have the same earth's curvature, so a trapping layer exists wherever $dM/dz < 0$. Therefore, this value can be considered the upper limit for ducting conditions. The values and regimes for M and N profiles are numerically compared in Table 2.

Refractive condition	***dN/dz* (*N* units/km)**	***dM/dz* (*M* units/km)**	**Radio horizon**
Subrefraction	$0 < N$	$157 < M$	Reduced
Normal	$-79 < N < 0$	$78 < M < 157$	Standard
Superrefraction	$-157 < N < -79$	$0 < M < 78$	Increased
Trapping	$N < -157$	$M < 0$	Largely Increased

Table 2. Comparison of N and M gradients for refractive conditions

The upper boundary of a duct will always be the top of the trapping layer. In the bottom, it can extend to a lower layer where reversed gradients may be found, forming then an elevated duct, or all the way down to the surface, then called a SBD.

The minimum trapping frequency f_{min} depends on the thickness of the duct d, which is equivalent to the height of the top for a SBD, also known as Z^*, in the case of Evaporation Ducts (EVDs). Although not a hard limit, frequencies below that value are less likely to be trapped, and it can be calculated with the empirical relationship (Davidson, 2003, p. 3-19):

$$f_{\min} = \left(\frac{3.6 \times 10^{11}\,\mathrm{Hz}}{\mathrm{m}^{-3/2}} \right) d^{-3/2} \tag{3.7}$$

Ducts are tactically significant, not only because RF systems may achieve longer ranges than expected, but there may also be "holes" where no signal will be present. RF waves, like the optical, can be prevented from propagating in some spaces creating a shadow effect, which severely limits the detection of targets in the area immediately next to the trapping layer because of the shadow effect. Although some scattering and diffraction can also be present, this can happen when the detecting system (such as radar or ESM) is above, below or in the trapping duct, and the target to detect is in a different

relative position, that is below, above, or out of the duct respectively, depending on the duct (layer) type occurrence. Therefore, for operational purposes, it is essential to determine the layering structure, the existence of layers and ducting, and if so, their thickness and heights.

As explained previously, this can be easily done by determining the *M* gradients, which can be obtained by

$$\frac{dM}{dz} \cong 124.6\ \mathrm{km}^{-1} - 1.57\ \mathrm{km}\cdot\mathrm{K}^{-1}\frac{dT}{dz} + 4.5\ \mathrm{km}^{-1}\left(\mathrm{mb}^{-1}\frac{de}{dz}\right) \tag{3.8}$$

This equation shows that, for a trapping layer to exist there must be large positive T gradients, and/or negative humidity gradients. Although such conditions can exist in any level of the troposphere, normally the largest gradients are achieved in the top of the Boundary Layer (BL). This is usually about 100-200 m from the surface, because of the strong mixing of water vapor and temperature profiles (either thermally or wind generated), so elevated ducts are commonly expected at that level. Additionally, ducts can be created and/or enhanced by subsidence (since the upper air parcels are dryer and raise their temperature adiabatically when descending, contributing both to increase *dM/dz*, and thermal inversions (for example, due to the cooling of soil during the winter nights).

However, ducting conditions are more likely above the oceans and other large water bodies since the water vapor source produces high HR values at very low levels (in which case they can create an known as evaporation duct EVD, sometimes up to 100% just above the surface.

On the other hand, some synoptic patterns can produce subrefraction. This is likely to occur in low level thermal inversions within a fully saturated layer, such as the advection of warm saturated air over cold waters, and can be strong in the warm sector of developing frontal systems. In those cases, there may be a reduction in the radar horizon, and significant probability of fade outs related (Goldhirsh et al., 1994).

Ducting conditions can be significantly different over the ocean than those over land because of diurnal heating, turbulence, and water vapor sources. Therefore, to analyze the feasibility of layering conditions in any specific area, there are several relevant factors involved that must be assessed, such as water surface temperatures, synoptic patterns (for example, the presence of high pressure air masses, and absence of low pressures associated with convergence), coastal breezes, and cloud patterns (in this case, looking for evidence of potential layering, such as strong negative gradients of humidity at the top of low level clouds).

C. VARIABILITY AND MEASURABILITY OF METOC FACTORS

As discussed, refraction of VHF/UHF/Microwave frequencies is primarily affected by the vertical gradients of pressure *p*, temperature *T*, and water vapor *WV,* which can by accounted for by the partial vapor pressure *e*. Since only the troposphere (usually heights below 10 km) shows significant gradients for these parameters, and the main interest of this study is surface surveillance and a ships' self defense, it will focus on the propagation anomalies for radar bands in the lower atmosphere.

To relate those variables with the *n* index, Deybe derived the equation

$$n \cong 1 + r\frac{2p\,A}{M}\left[a + \frac{m^2}{3kT(1+iwt)}\right] \tag{3.9}$$

where *?* accounts for the density of air, *A* is the Avogadro's number, *M* is the molecular weight, *a* is the polarizability coefficient, μ is the permanent electric dipole movement, *k* is Boltzmann's constant and *T* is absolute temperature (in °K), $w = 2p\,f$ (being *?* the frequency of the external field), t is the time required for external field-induced orientations of the molecule to return to random distribution, and $i = \sqrt{-1}$ (Davidson, 2002, pp. 3-6, 3-7).

It shows that dependence on frequencies above 100 GHz is negligible because $it \ll 1$. For frequencies between 100 MHz and 80 GHz, the refractivity *N* can be computed by the equation

$$N = 77.6\frac{P}{T} - 5.6\frac{e}{T} + 3.75\left(10^5\frac{e}{T^2}\right). \tag{3.10}$$

In the atmosphere, the most significant changes of N occur in the vertical dimension, and the degree of refraction is related to N gradients, rather than the absolute values, so using the standard gradients for P, e and T, this expression can be derived to be:

$$\frac{dN}{dz} = .27\left(\frac{dP}{dz}\right) - 1.57\left(\frac{dT}{dz}\right) + 4.5\left(\frac{de}{dz}\right)\left[\mathrm{km}^{-1}\right]. \qquad (3.11)$$

It gives approximate values of dN/dz = -40/km, with typical values for N between 300 and 400, with approximately 315 as the normal value according to the ITU, under a US standard atmosphere of 15°C at 45°N (Skolnik, 2001, p. 499), but this is clearly not the case for the Northwest of the Caribbean Sea.

One important implication is that for cold air masses (low T values) the contribution of water vapor is also relatively small because, even when saturated, the partial vapor pressure is small. On the other hand, the direct relationship between the temperature of warm air masses and their ability to hold more water vapor has a stronger influence in the refractivity gradients. Thus, anomalous refraction is more likely in maritime tropical air masses because of their larger water vapor contents.

In principle, the propagation of EM waves through the atmosphere and its anomalies could be properly evaluated if the exact composition of the atmosphere along the path of interest would be determined. Those measurements must be both precise and time frequent enough to ensure that they truly represent the atmosphere intended to be described.

However, in the littoral environment, the parameters used to predict the propagation patterns are highly variable because of differential advection of horizontal contrasts, and coastal wind circulations. Despite the fact that they can radically change in a few hours, the availability of data sources can limit its analysis to a day-to-day basis. Thus, for shorter terms evaluations, the operational problem is how to determine effectively when and where layering conditions may exist.

There are basically two methods to gather data for determining refractivity profiles: radiosondes (with several variations, such as dropsondes, and rocketsondes), and

refractometers. The latter is very precise, but too costly, and not operationally as suitable as the former methods might be. On the other hand, evaporation ducts cannot be easily detected by radiosondes. Their typical vertical resolution is about 50 m, and the strongest surface gradients are below that, so the radiosonde data smoothes them (if detected) because it cannot resolve them, thus misleading the predictions.

In any event, these evaluations are mostly made under the assumption of homogeneity of the atmosphere, that is, the data gathered at the monitoring stations is considered also valid for the ship's location. Yet this is seldom true, because the environment can present highly variable characteristics that can compromise the results of those systems. Some modern warships have implemented automated data collection platforms, including the use of rocketsondes and floatsondes when required, to continuously sample the environment so they can provide high resolution data for the computer assisted TDAs to predict refractivity conditions.

Anyway, this can only be done for the local operation area of the ship, and further research of remote sensing options is still required (Whalen, 2002). In the horizontal dimension, there may be significant differences between sea and land profiles, but such profiles can also change greatly over time. Therefore, both spatial and time resolution of data might be improved by using data from other platforms, such as buoys, surface stations, other ships, satellite derived data, and eventually, the outputs of computer models.

Previous radar propagation studies have usually assumed independence of the azimuth direction, unless the radar ranges are very large. Since ducting and abnormal refractivities can normally be associated with stable conditions, while for the horizontal gradients to be significant there must be certain turbulence and unstable conditions, it seems to be a reasonable assumption. Nevertheless, for this assessment to be accurate, it assurance is needed that the horizontal gradients of T and WV are not significant, and when the area of interest includes the shore line and strong local effects (such as orographic influences and sea-land breezes), that homogeneity cannot be taken for granted, particularly for LW purposes.

IV. SCOPE AND APPROACH

This study is aimed at evaluating the effects of meteorological METOC factors on the expected performance of EW systems against low detectable targets in a specific tropical littoral region. To evaluate the EM propagation, the relevant characteristics of climate and weather in the area of interest and their variability are presented. Then, they are used to define three case studies, framed on a short term (day to day) basis with respect to different influencing weather patterns with available data for he year 2003. Further, it analyzes the applicability of the obtained results from atmospheric propagation models for LW operational purposes in a warm water environment.

A. EVIDENCES OF DUCTING AND ANOMALOUS EM PROPAGATION

As previously discussed, evaporation ducts are extremely relevant in EW, because the relative location of the target and the radar antenna can be crucial for the enhancement (or prevention) of detection.

It was also shown that the minimum trappable frequencies are related to the duct's thicknesses. Ducting conditions are more persistent over the warmer subtropical and tropical oceans than those over land or in high latitude ocean storm track regions because of the characteristics of their associated air masses. Previous studies (Ortenburger, 1973) produced ducting statistics for various areas of the world, showing the Tropical Eastern parts of Pacific and Atlantic Oceans, upper Indian Ocean and the Persian Gulf as the most prevalent ducting regions. However, there is climatological data that shows the average conditions for the Eastern Caribbean with evaporation duct heights (Z^*) from 10-24 m for about 30% of the time, and up to 30 m or more for almost 20% (Davidson, 2003, p. 5-9). This happens mostly because the warmer sea surface temperatures enhance the capability of adjacent air masses to hold water vapor.

The existence of layering conditions aloft can also be directly associated with the characteristics of air masses in the tropics and their interactions; for example, when tropical maritime air masses with moist lower levels and dry overlying air occur; or when

continental air masses, certainly dry, flow out over the cooler water surface so they present a thermal inversion and associated dry layer in upper (not necessarily too high) levels.

The influence of land-sea breezes can increase the duct thickness, although their interaction with major synoptic and mesoscale events and their associated features may clearly modify the regular propagation patterns. This is significant because the range of affected frequencies will typically be from X (I/J) band (10 GHz), down to S (E/F) band (3 GHz) and lower, which include the frequencies normally used by shipborne radars for tracking and surveillance, respectively, and their detection capabilities can thus be severely modified.

B. GEOGRAPHIC LOCATION

The area of interest for this study is the Yucatan Channel, due to its strategic importance and relevancy of the inherent METOC scenarios in its geographical location. This is a passage 190 km (105 nmi) wide between Cuba and the Yucatan Peninsula, connecting the northwestern extremity of the Caribbean Sea with the Gulf of Mexico. It represents a high strategic value area because of the intense air and marine traffic converging on it; therefore, maritime interdiction and law enforcement operations are very important.

From the METOC point of view, this region has several unique geographical features. It is a region around 20°N (between Marsden Squares 45 and 81, from 85°W to 87°W), bounded by the Highlands of Central America in the South, and the Gulf of Mexico in the North. It is under the influence of the oceanic subequatorial current, with an annual average Sea Surface Temperatures (SSTs) above 27.5°C (GMCA, 2004) and the permanent Trade Winds, as well as the seasonally migrations of the intertropical zone of convergence (ITCZ), weather fronts, and tropical cyclones.

C. CLIMATOLOGY

Most of the available regional METOC studies address statistics for the Tropical Atlantic and Gulf of Mexico. Sometimes they refer specifically to the Caribbean Sea, but seldom to the Yucatan Channel. Since it is a boundary between the last two major regions, some climatological descriptions may apply in general, yet the variability and

local features differ from each other. For example, the Caribbean is supposed to have the best weather in winter, with rare gales, very good visibilities, and very infrequent showers (NAVAIR, 1985). On the other hand, in the Gulf of Mexico (near the area of interest) the winter is characterized by the incidence of many successive cold fronts, with high pressure air masses and variable winds commonly shifting from South and Southwest, to strong gales from North and Northeast after their pass.

According to the Köppen classification of world's climates, the Yucatan Peninsula is a "tropical wet-and-dry" region (Ahrens, 1994). The total rainfall fluctuates widely from one year to the next, usually from 100 cm (40 in) up to about 200 cm (80 in). There is a dry season where the monthly rainfall is less than 6 cm (2.3 in) for at least two months during the winter under the influence of subtropical highs, while during the summer, slow moving shallow lows that pass through the region enhance heavy precipitation, mostly in the form of showers. In contrast, Central America's annual averages range from 200 to 600 cm (80 to 240 inches), with the highest rates in the cloudy season from June to October, when sky cover equal to or higher than ¾ is observed about 18 to 24 days per month. The least cloudy months are March and April, with skies overcast approximately six to eight days (NAVAIR 50-1C-543, 1985).

Temperatures and humidity also have large variations with time, normally more over the course of the day than they do on average over the year. For example, relative humidity reaches 80-90% during the early morning hours throughout the year, with the highest values often occurring during fall and winter, and the lowest during spring. During the afternoons, those values fall into the 70% range. During the winter season, the maximum daily average of 30-32°C (86-89.6°F) can drop during the night to a minimum of 20°C (68°F) in the early morning, and down to 15°C (43°F) in the lowlands of Central America because of the combined effects of intrusions of cold dry air from the North and clear skies, allowing rapid radiational cooling (Williams et al., 1989). During the spring, the noon sun is higher, and the greater surface heating can easily produce temperatures above 38°C (100°F), creating hot dry conditions, that will be attenuated by cloud patterns and rain during the wet summer season, followed by a similar pattern in fall (Ahrens, 1994).

Trade Winds keep a well mixed boundary layer with large positive temperature and negative humidity gradients on top, called the Trade Wind inversion. This is expected to be at high levels in the western part of the oceans (up to 4,000-6,000 ft., before dissipating), so it would not be a significant factor for low level layering in the Yucatan Channel. The existence of surface ducts must be related to other issues, although the trade winds can play an important role when interacting with local features.

In the low latitude tropics, streamlines of wind field contain the most information. This arises because of small gradients of pressure and low Coriolis acceleration, so streamlines and isotachs are a key in tropical analysis (Jeffries et al., 1992, p. 28). Dominant winds are normally from the East, regularly disturbed in some degree by the more defined easterly (tropical) waves, and more clearly by northern winds associated with cold fronts from October through April.

1. Fronts

Frontogenesis is usually associated with extratropical cyclones in higher latitudes, but during the winter, cold fronts do extend to lower latitudes. They produce big horizontal gradients of *T, P,* and *HR*, as well as weather features that can be associated with some refractive conditions, such as cloudiness, fog, or rain.

When a front approaches, high pressure and associated subsidence after their pass are very likely to produce layering patterns. Dynamics on cold fronts are expected to disrupt stability patterns just ahead of the front line and no layering can be observed. Yet, the low level through is associated with an upper ridge, which can produce strong inversions because of subsidence in the adjacent areas behind the front. It is difficult to determine an exact number of expected “northers” in the region, but there are estimates of about 30-40 events per year (Williams et al., 1989, p. 1-27). On the other hand, warm fronts are more related to stable conditions, so the thermal layering should also be analyzed to find probable subrefractive conditions, because of the prefrontal “steady” conditions of warm and moist.

2. Tropical Cyclones

Easterly waves affect the region with the occurrence of clouds, showers, and thunderstorms, most frequently during summer and fall. They are a significant source of rainfall for the Caribbean, and if unstable enough, they can develop into tropical cyclones.

Tropical cyclones are normally a threat from June to November, with a higher probability in June and July in the Gulf of Mexico. By August, there is a chance of 10-20% having a tropical storm or hurricane, most likely near the Yucatan Channel, which increases during the fall to 15-25% probability of a hurricane from September to October (NAVAIR, 1985).

Based on statistics from 1887-1955, in the North Atlantic, there is an average incidence of 7.5 cyclones per year, with 3.8 of them reaching hurricane intensity although more recent statistics during the past 34 years of data indicate an average of 9.8 cyclones (Asnani, 1993, p. 740). The storm paths tracked by the National Hurricane Center of Miami, Florida during the last ten years, show 21 cyclones in the Yucatan Channel: four tropical depressions, nine tropical storms, and eight hurricanes.

Tropical cyclones usually last only a few days, so their effects are hardly reflected in the climatological databases, but they are extremely important in the weather conditions for the area. Despite the relatively short duration, the severity of their effects may clearly affect the EM propagation characteristics in operationally critical moments. They can be associated with up to 5°C of cooling the SST by upwelling and wind enhanced evaporation after their pass, as well as the relative drying of air near the surface due to associated subsidence out of the center, going from nearly 100% in the cloud walls around the eye, to about 75% in a radius of nearly 90 km, as well as beyond 300 km from the center in a mature hurricane (Asnani, 1993, p. 786).

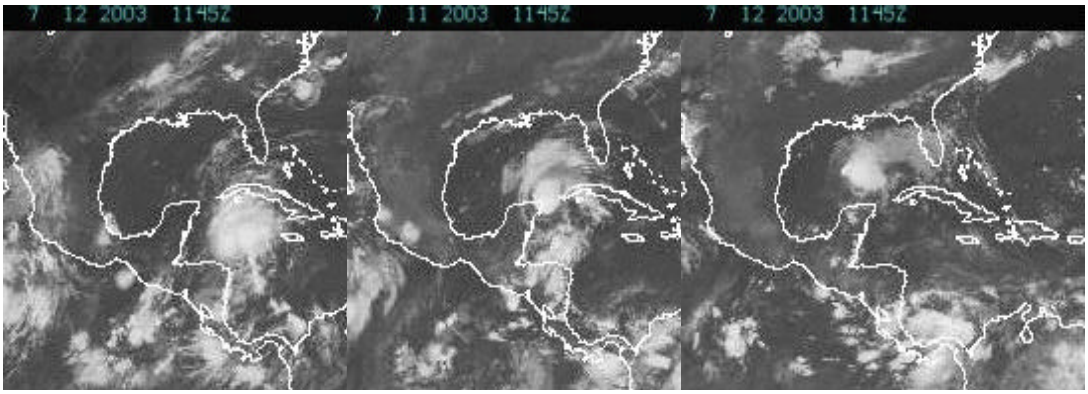

Figure 4. Satellite images showing tropical storm Claudette in the period 10-12 July, 2003 (After NOOA, Tropical Prediction Center, 2004)

3. Local Features

When no major synoptic features are present, the general synoptic conditions are rather smooth (except for tropical cyclones incidences), and the local airflow patterns become more important. This is expected to occur during the spring and fall, generally considered as "transitional seasons."

Periodic daily processes and circulations on the local to mesoscale dominate the regional climate and weather in the tropics. In the time scale of a day or less, horizontal contrasts in the surface heat budgets and thermal tides yield vigorous circulations which dominate the diurnal cycle of cloudiness and rainfall. Diurnal wind reversals can extend up to 100 km inland. Although not sea breezes in the classical sense, their interactions with other local circulations and major synoptic features, such as the trade winds, can result in complex changing features (Hastenrath, 1985, p. 6).

Local wind patterns can be related to diurnal land-sea breezes. The Yucatan Peninsula is a large flat area, with low vegetation, but the shape of the peninsula enhances the divergence-diurnal occurrence associated with land-sea breezes, and this can be expected to enhance the layering conditions above the Channel waters. Under extreme conditions, the ducts might be very strong, and the relative location of the EW systems can prevent the detection of small targets.

D. METOC DATA SOURCES

Previous studies have provided climate values for this area, and they have been analyzed in detail because of its importance to economic and political activities.

However, operational METOC data collection platforms are rather heterogeneous with regard to coverage, and their databases are not necessarily compatible, which complicates the scenario definition.

For the purposes of this study, the representativity of upper air soundings is very important, since regions of extreme conditions with important operational implications may not have profiles to examine the effect of METOC on EW. Additionally, radiosondes do not have enough resolution to describe evaporation ducts, so detailed surface data of air temperature, humidity (*WV* content), pressure, wind, and SST is required; hence the importance of having reliable local surface data (ideally from buoys) to describe the actual conditions at sea, and the lower atmosphere in the area.

There are no operational moored buoys in the area, and even though the intense maritime traffic provides several ship reports, these are not periodical and their SST readings not very reliable. As a consequence, it is not easy to identify offshore weather patterns such as diurnal breezes, and hourly changes in temperature or humidity. Since those are important factors to describe atmospheric propagation characteristics of EM waves, this study also addresses the feasibility of complementing data from alternative data sources, and the added value of such data when used with a TDA in an operational environment.

E. APPROACH

1. Data Bases

The area of interest has three radiosonde stations: Grand Cayman Island (WMO Id. 78384), and the International Airports of Cancun (WMO Id. 76595) and Belize (WMO Id .78538). Although all of them are coastal, their local conditions are not similar, so the resulting evaporation ducts were radically different. In addition, they only produce soundings data once a day, at 12 Z, which prevents the possibility of identifying diurnal effects.

The radiosonde station of Cancun (Figure 4) was chosen for this study because of its convenient position for operational purposes in the Yucatan Channel, low elevation above MSL and proximity to the coast line, as well as the availability of surface data in the area from weather stations of the Mexican National Weather Service Automated

Weather Stations Networks in Cozumel, Cancun, and Sian Kaan, and from the Mexican Navy (in Isla Mujeres), which also has a tidal station in Cozumel that provided some actual values for SST.

Figure 5. Area of interest and location of stations

All these surface stations are automated, so they provide high accuracy and temporal resolution, but this also presented some drawbacks. They relay their data to Mexico City via satellite telemetry which caused several gaps in the databases. Besides, all this was raw data, never validated or subject to further processing for quality control, so it was individually evaluated by comparison between stations (when available). Several batches of suspicious data from those databases had to be discarded and a more rigorous statistical evaluation was not possible.

Despite these problems, there was excellent agreement between stations in the overall trends for the gradients shown, which allowed extrapolating some values when needed for each case. There was also a very good agreement between the averages calculated from the available data and the extensive climatological database from the U.S. Navy "Global Marine Climatic Atlas" (GMCA, 2004). This atlas was derived from data collected primarily from ships for the period from 1854 to 1997, which was processed for quality control and collation from the Comprehensive Ocean and

Atmosphere Data Set (COADS) distributed by the National Center for Atmospheric Research (NCAR). This provided a good guidance for supporting the approach used in each case study and the validity of the outcomes.

2. Propagation Model

The Advanced Refractive Environment Prediction System (AREPS) was developed by the Atmospheric Propagation Branch at the Space and Naval Warfare Systems Center, San Diego. It uses the Advanced Propagation Model (APM) to calculate range-dependent EM system propagation loss within a heterogeneous atmospheric medium, where the index of refraction is allowed to vary both vertically and horizontally while accounting for terrain effects along the path of propagation.

In this study, AREPS was used to evaluate individual responses to changing input parameters, according to observed environmental conditions. The required input sets were completed with data from several coastal weather and tidal stations, ships and buoys reports, when available.

3. AREPS Statistics

AREPS also includes numerous statistics of tropospheric ducts and super-refractive layers compiled by GTE Sylvania, under contract by the Department of Defense. They are the result of a large-scale analysis of a five year database with approximately three million worldwide radiosonde soundings from 921 observing stations (Ortenburger, 1985). Only soundings which included surface data were analyzed, but the statistics show monthly occurrences for elevated ducts and for SBDs, not necessarily evaporation ducts (EVDs).

For the surroundings of the Yucatan Channel, there are statistics only from the radiosonde station of Merida, Mexico (WMO Id. 76444), which is an inland station about 20 miles South of the nearest coast, and 11 meters above mean sea level. They show more SBD occurrences from July to October, with a maximum of approximately 30% of the time in September (Figure 5). When that analysis was made, soundings from Merida were available twice a day, at 00 and 12 Z, so the statistics could be split into day and night occurrences (about 1800 and 0600 hrs, Local Time).

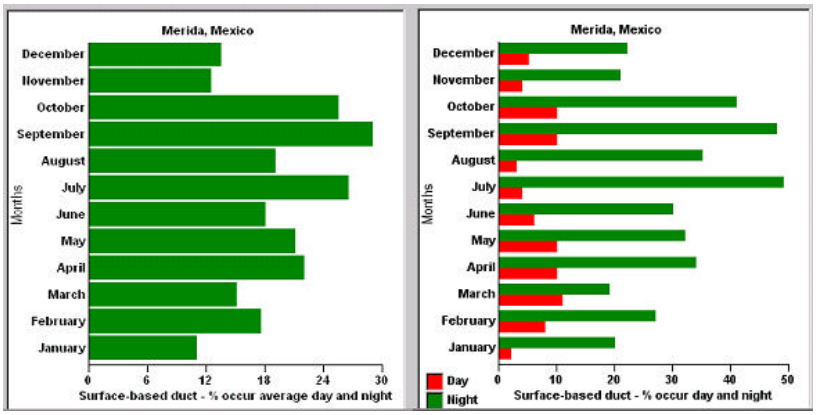

Figure 6. Statistics of SBD monthly occurrences for Merida, Mexico (WMO Id. 76444) from AREPS

It can be seen that evening ducts occurred much more frequently in August and September (up to 50% of the time), and significantly less in the mornings, particularly in January, July and August. These are evident seasonal and diurnal signals, which may be important for operative purposes since the METOC factors involved can induce large changes in the ducting and layering profiles, modifying the EM propagation patterns.

4. Climatology of Evaporation Ducts

Evaporation ducts and their effects in surveillance and detection operations in the maritime surface are very important for the purpose of this study, but AREPS does not have climatological data for the area of interest. Thus, a separate analysis was done with monthly surface climatology data from the GMCA and using the NPS model (included in AREPS 3.3) to build the refractivity profiles of April, December and July (Figure 6).

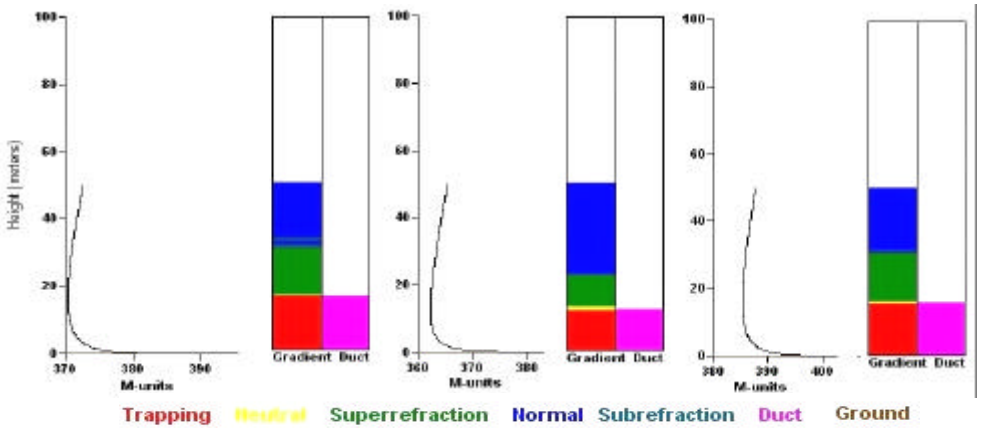

Figure 7. Evaporation duct profiles for April, December and July, calculated by AREPS with monthly climatological data from the GMSA

The resulting profiles showed EVDs with average values of Z^* about 12.6 m for December, and 16 m for both April and July, which may be expected to produce extended ranges for frequencies above 4 and 8 GHz respectively. The relationship between the Z^* values, SST and the Air-Sea temperature differences was also evident, such as the thinnest EVD with the coolest SST and the most negative temperature difference in December, as expected, which is shown in the Table 3.

	Jan	Feb	Mar	Apr	May	Jun	Jul	Aug	Sep	Oct	Nov	Dec	Annual
Air Temp	24.4	24.4	24.3	25.7	27.17	28.11	28.6	28.4	27.84	26.4	24.7	23.1	26.09
SST	26.1	25.8	25.2	26.2	27.55	28.37	28.9	28.8	28.48	27.5	26.2	24.9	27
Air-Sea Temp. Diff.	-1.7	-1.4	-0.9	-0.5	-0.38	-0.26	-0.3	-0.42	-0.64	-1.1	-1.5	-1.8	-0.91

Table 3. Values for Air-Sea Monthly Mean Temperatures difference, from the Global Marine Climatic Atlas

This proved to be an interesting consideration, whereas those are results for monthly averages from long term climatological data, yet the local factors, diurnal variability, and synoptic features are still expected to play a major role in the variability of the propagation characteristics, as previously discussed.

THIS PAGE INTENTIONALLY LEFT BLANK

V. RESULTING EM PROPAGATION PROFILES

A. CASE STUDY 1: SPRING SEASON

Spring is considered a "transitional" season, that is, with low gradients of the meteorological variables and not much variability can be expected in the refractivity profiles, since there are no significant weather features other than local small scale effects (Figure 7).

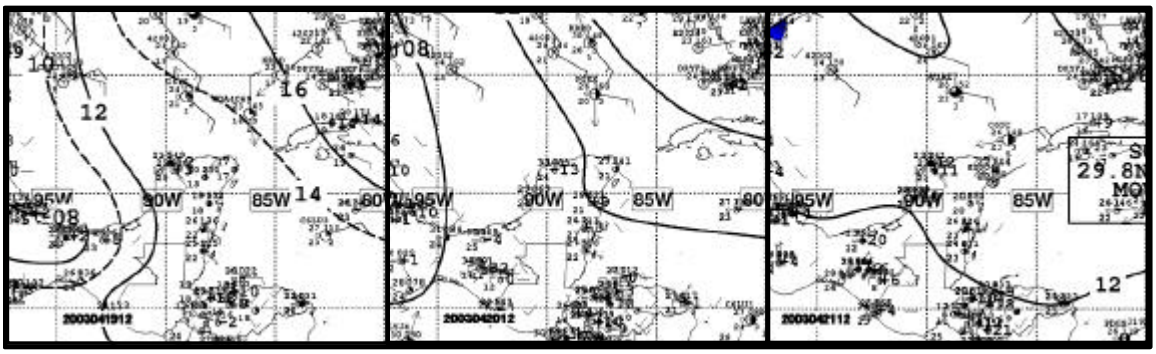

Figure 8. Synoptic Analysis at surface level from 19-21 April, at 12 Z (After NOAA Tropical Prediction Center, 2004)

The overall conditions for sea and air traffic appear to be optimum, as well as those for naval operations, such a scenario may be thought of as an ideal one, useful to get a frame of reference with which to assess the modifications when abnormal refractive profiles are found, and compare them with those for a standard atmosphere (Figure 8).

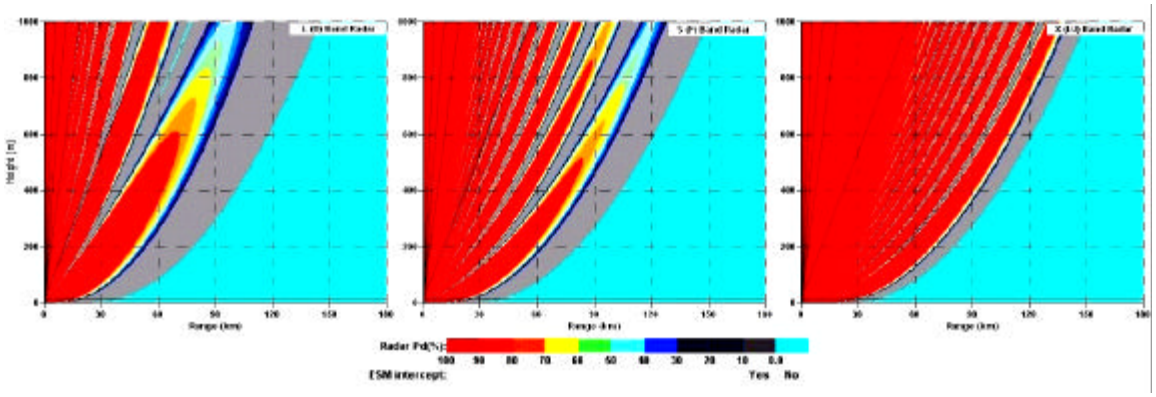

Figure 9. Normal propagation patterns for L, S and X band radars under a standard atmosphere

Nevertheless, a more careful approach showed that the existing atmospheric and oceanographic conditions, such as warmer air and SSTs (refer to Table 2 in the previous chapter), could be related to enhanced ducting and trapping conditions, so the RF scenario might be not as ideal. Electronic surveillance performance and situational awareness may be unknowingly modified, and a more precise assessment of the effects would then be needed.

1. Diurnal Changes

In general, there were no major changes in the thickness of the observed EVDs, with average Z^* values near the climatological mean. However, the actual SSTs registered were nearly 1.5°C above the mean of 26.7°C, which resulted in slightly thicker ducts than the "normal" mean value of 16.4 m. During the three day period of 19-21 April, there was an overall diurnal variation of Z^* about $\pm$ 2 to 3 meters, with maximum values up to 17.8 m in the evenings. These ducts are very likely to modify the propagation of frequencies above 4 GHz with extended ranges for transmissions below the duct top, but also reducing the detectability of targets just above this duct.

A similar effect in the detection ranges was also produced after the expected thickening of the EVD in the evening of 20 April (at 1800, Local Time), as shown in Figure 9. This was observed only when the radar antenna was pointing offshore (true bearing 135°), and not inland (true bearing 270°), because AREPS was able to suppress the EVD over the ground effectively, thus making an obvious difference between waves propagating over the sea and over land (Figure 9).

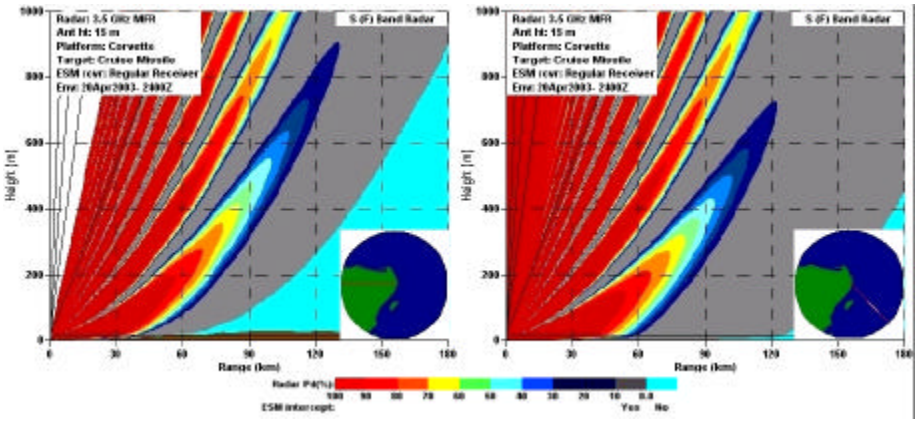

Figure 10. Expected propagation patterns for an S band radar pointing inland (left) and offshore (right) with surface data for 20 April at 24 Z (1800 LT)

2. Changes in Antenna Heights and Radar Frequencies

In the evening of 20 April the EVD height was increased more than 3 m from the 12 Z value (to 17.6 m), which was now expected to modify the propagation of frequencies above 4 GHz, although this height is also similar to usual antenna heights for many naval radars. When the antenna heights were increased from 10 to 20 m, the resultant ranges were also increased due to extending the radar horizon, but this was observed to be really significant only for the X band radar (higher frequencies), whose detection ranges at surface levels where almost doubled from 30 to about 60 km.

It was also noticed that the increase of Z^* to more than 17 m in the evening, was large enough to show its effects on the S band when the antenna heights were changed. In this case, however, the most evident difference was not in surface range increases (which were only about 10 or 20 km), but reducing the overall achievable range in the lowest lobes with respect to those with a standard atmosphere.

The resulting profiles proved to be particularly sensitive to the different combinations of frequencies and antenna heights, so the outcomes are not easy to predict. Thus, only long term runs, with more accurate data, may produce a reliable guidance for operational predictions of the achievable performances under such conditions.

3. Day to Day Changes

On a day-to-day basis, a more important variability was observed when the appended profiles showed the evaporation ducts embedded in significant SBDs. Since the synoptic variability of the M gradients were actually small, the observed variability in the bottom part of the profiles was more "sensitive" to the evaporation duct or surface data. As a consequence, the resulting SBD may be largely variable, such those from 19-21 April displayed in Figure 10, where SBDs of 50 m exist at the beginning and end of a 48-hour period above a persistent evaporation duct of nearly 15 m throughout. If these profiles are proven to be realistic, then their effects in the propagation patterns can be severe for almost any system using frequencies above the L band (1 GHz).

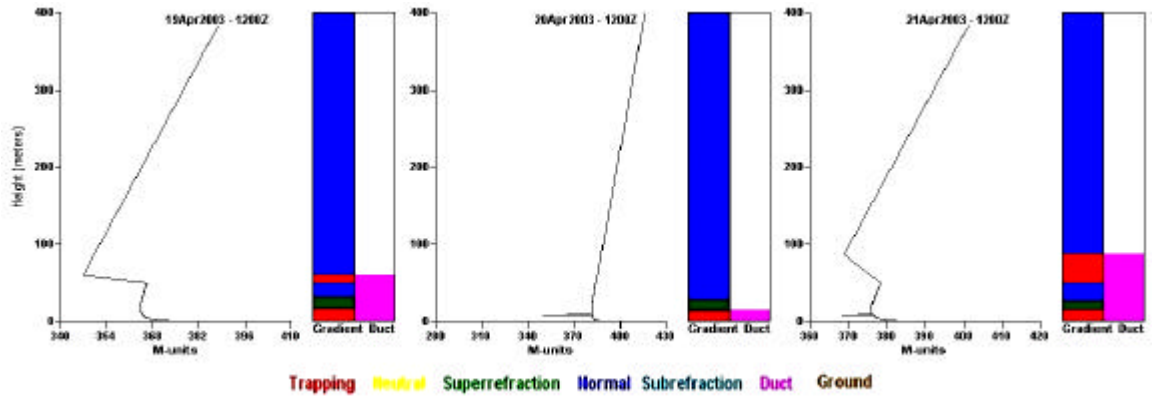

Figure 11. Resulting profiles from appending surface data to the 12 Z radiosondes for 19-21 April, respectively

Figure 11 shows how those SBDs were thick enough (60 and 87 m, respectively) to significantly affect most radar frequencies with dramatically increased surface detection ranges, well beyond 180 km (100 nmi) within these ducts, while also severely degrading the detection capabilities in the layers between 100 and 400 meters (down to less than 30 km), where ranges between 60 and 90 km would be achieved under a standard atmosphere.

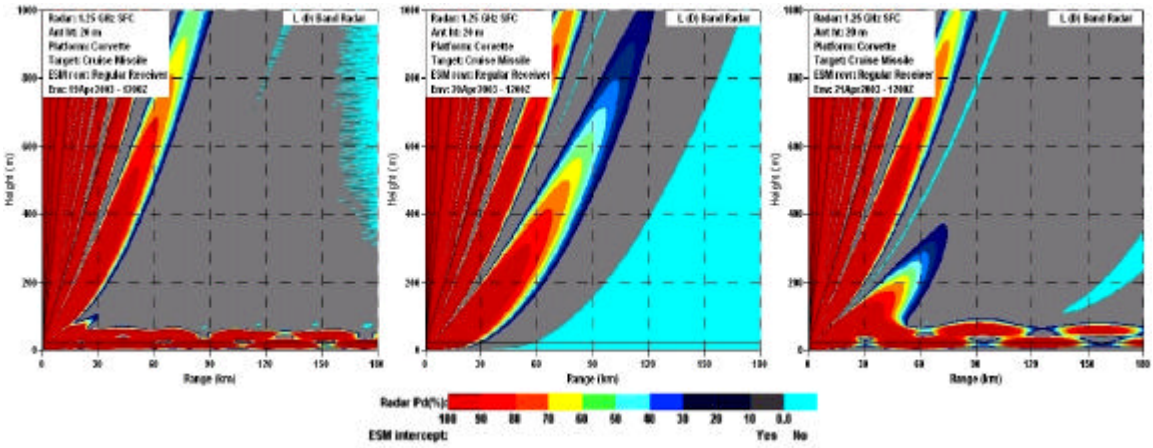

Figure 12. Propagation pattern for a L band radar, with 12 Z profiles for 19-21 April

For MFRs, this may be a serious limitation in detecting low flying aircrafts, combined with a false "awareness" of the operators produced by much better performances on surface detection, or greatly enhanced clutter that may lead to increase the filtering, hence reducing the sensitivity of the radar to detect small sea skimming targets effectively. Since the energy of the transmitter is severely prevented from

propagating through those areas, there is also a large limitation in the detection capabilities of passive ESMs, and they cannot detect any transmitter at those frequencies in large areas where they normally could.

One interesting effect appeared in the X band radar when scanning above land (true bearing 270°), as shown in Figure 12. In this case, the tracing of rays showed many narrow lobes escaping from the SBD in a somewhat random manner, apparently because AREPS neglects the EVD effect inland. They created a wide spread area of "noisy" detections, which may be confusing for the operators and/or automated systems, since normally there would not be any signal echoed from that area, and the signal processors may be troubled by such effects as well. Whether or not this is a feasible result should be proven under more rigorous and precise data, with better resolution in time and space.

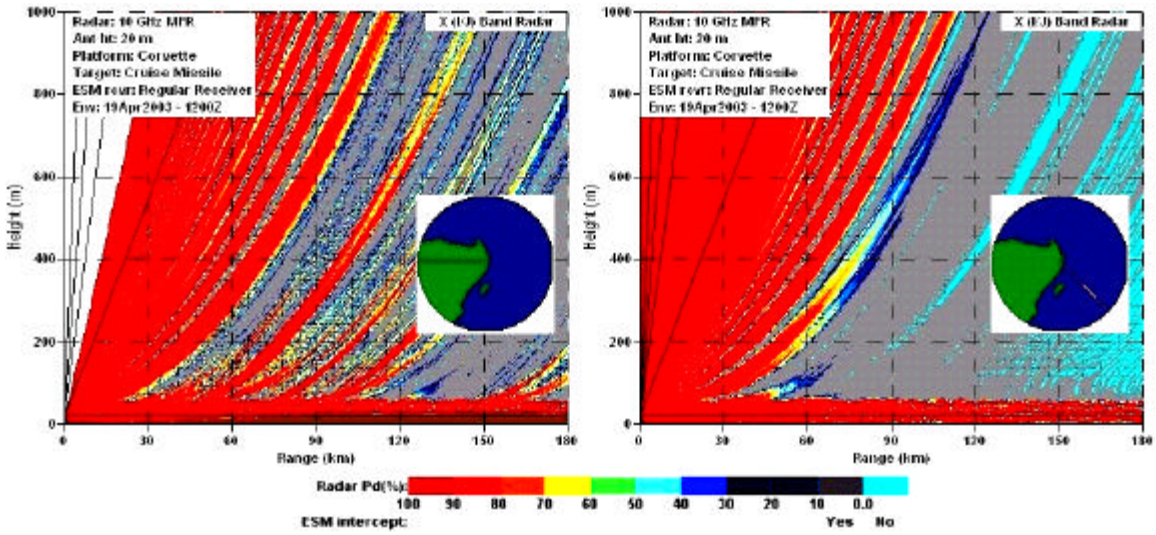

Figure 13. EVD effects for an X band radar on 19 April, at 12 Z, when scanning inland (left) and offshore (right)

B. CASE STUDY 2: COLD FRONT CONDITION

From October to April, the mean monthly value for SST goes down to 24.9°C, but the air temperature becomes even cooler, so the ASTD can reach maximum values of almost 2°C (refer to Table 2 in Chapter IV). Further, this region is frequently affected by cold fronts with strong winds and high pressure air masses, which repeatedly appear in the area with only a few days of separation. Although their occurrence is highly predictable, these systems can move fast enough to sweep an area such as the Yucatan

Channel and disrupt the local refractivity profiles in a matter of only a few hours, so the radiosonde data available every 24 hours is not enough to describe the changes in such profiles. Therefore, a better understanding of their effects would be highly beneficial to optimize the performance and use of EM equipment.

The climatological profile for December (Figure 14) indicated a normal Z^* of 12.6 meters, which can be expected to produce extended surface ranges for frequencies roughly above 8 GHz. The available data for the period from 23-26 December showed actual SST nearly 1.5°C below the monthly mean, which was reflected in thinner ducts with lower Z^* by as much as 3 meters, and the expected band of affected frequencies would then be higher (only X band or above).

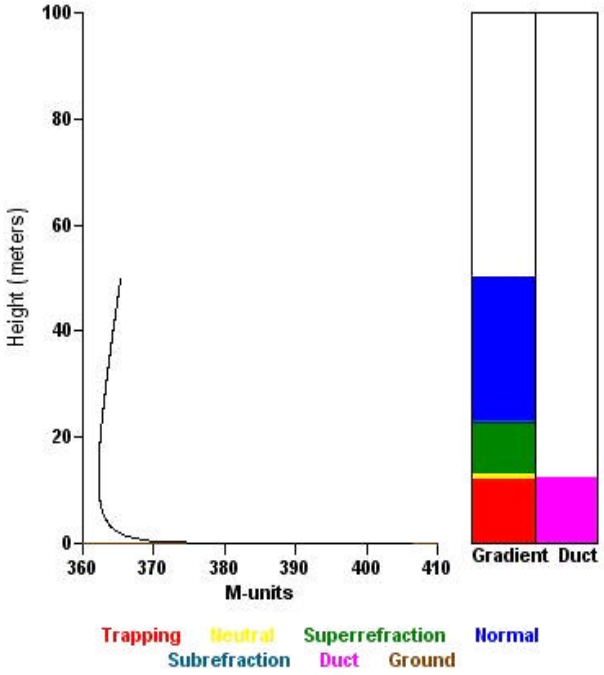

Figure 14. Climatological profile of refractivity for December for low levels, after

Surface analysis showed a front cold reaching Cancun on 25 December (Figure 14). Although the Skew T plots of the daily radiosondes at 12 Z (Figure 15) and the surface data did not clearly show the exact moment when the front passed, they gave some evidence of its effects as the system moved over the area.

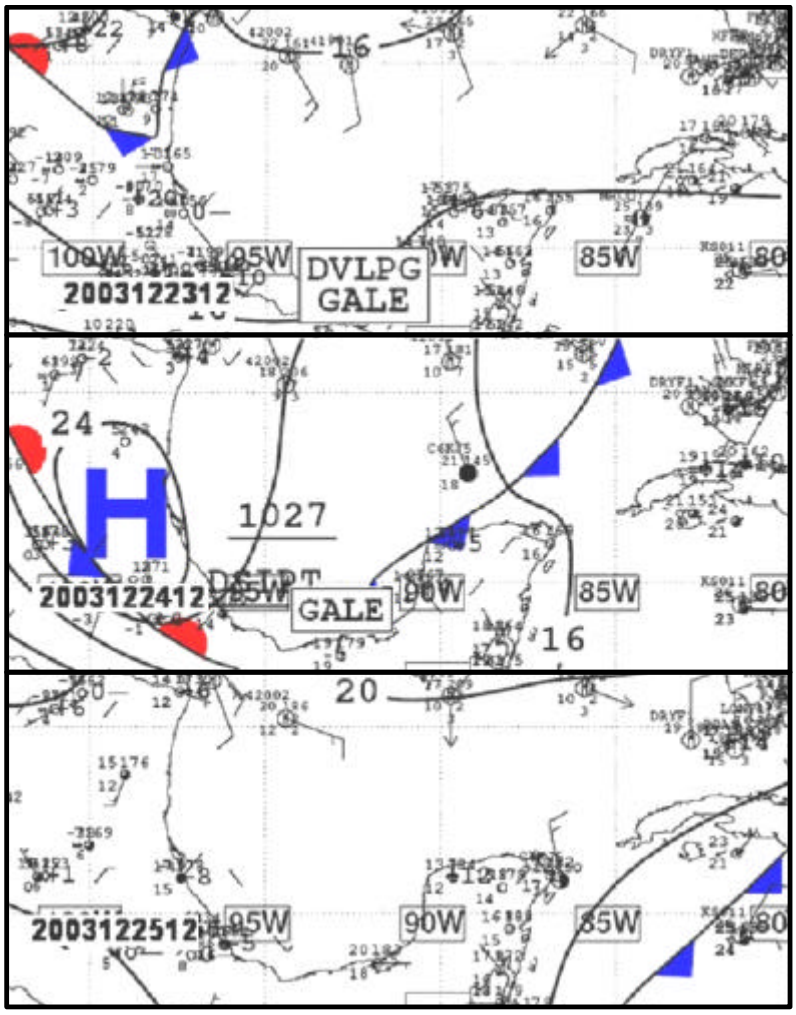

Figure 15. Surface Analysis for 23-25 December at 12 Z, showing the pass of a front cold over the Yucatan Peninsula in less than 24 hours (After NOAA Tropical Prediction Center, 2004)

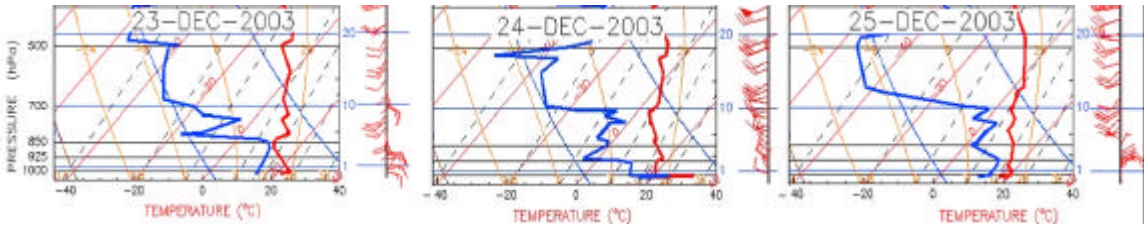

Figure 16. Skew T plots of the radiosonde data for 23-25 December, at 12 Z, showing the pass of a front cold (After NOAA Forecast Systems Laboratory, 2004)

To analyze its effects, surface data was appended to the radiosonde data, and then used to build the refractivity profiles. It must be recalled that this might produce unrealistic results about the presence (or absence) of actual SBDs because of using

outdated upper air data, particularly for the evening profiles. Instead, they should be used as a reference to evaluate the variability of the profiles in the lower levels. For example, the observed evaporation ducts were thinner than 10 m (Table 4), so a reduced detectability of low surface targets, such as small boats or sea skimming missiles may be expected from radars with antennas at normal heights of 15 m.

Date	Z*	Top of SBD
23Dic2003	19.4	68
24Dic2003	6.9	*
25Dic2003	9.0	110
26Dic2003	3.4	172
27Dic2003	18.3	85

Table 4. Heights of EVDs *(Z*)* and SBDs during 23-17 December, from appending radiosoundings and surface data with the NPS model included in AREPs.

Although there was an evident reduction in the *Z** value between 23-24 December (from almost 19.4 m, down to 6.9) before the depicted arrival of the front, the appended profiles shown in Figure 16 indicate thick layers with superrefractive profiles. As mentioned previously, low *M* gradients may easily cause AREPS to artificially detect (or neglect) SBDs, depending on the surface data appended, so these results must be viewed with some caution.

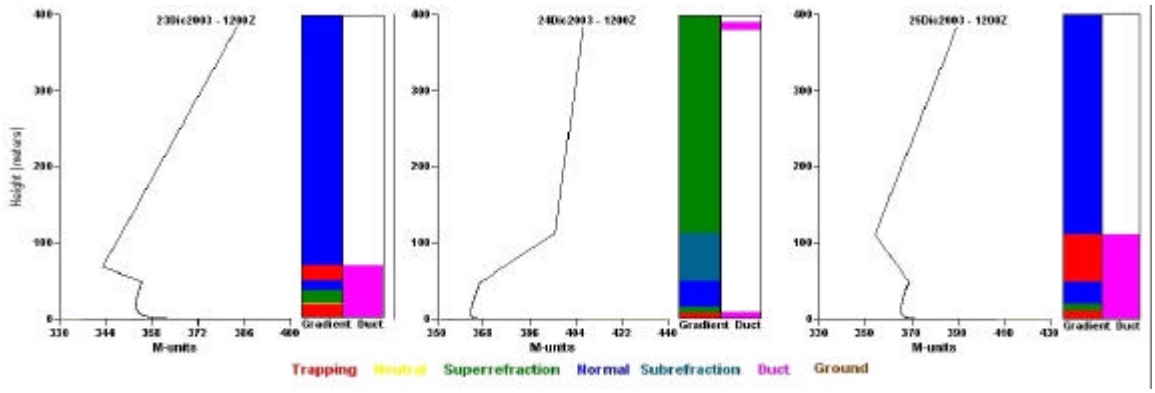

Figure 17. Refractivity profiles from AREPS, after appending surface data to upper air soundings for 23-25 December, at 12 Z

An important example was 23 December, when the propagation patterns showed a strong effect in the lower levels because of a SBD with a top height of 68 meters, thick enough to trap even the L band radar waves. As a consequence, there was a very extended detection range from the surface to the top of the duct of more than 180 km, altogether with significant reductions just above the duct, with respect to the normal pattern (Figure 17). Is also important to note that in this case, the EVD top height was slightly less than 20 meters, so changing antenna heights enhanced or reduced such effect.

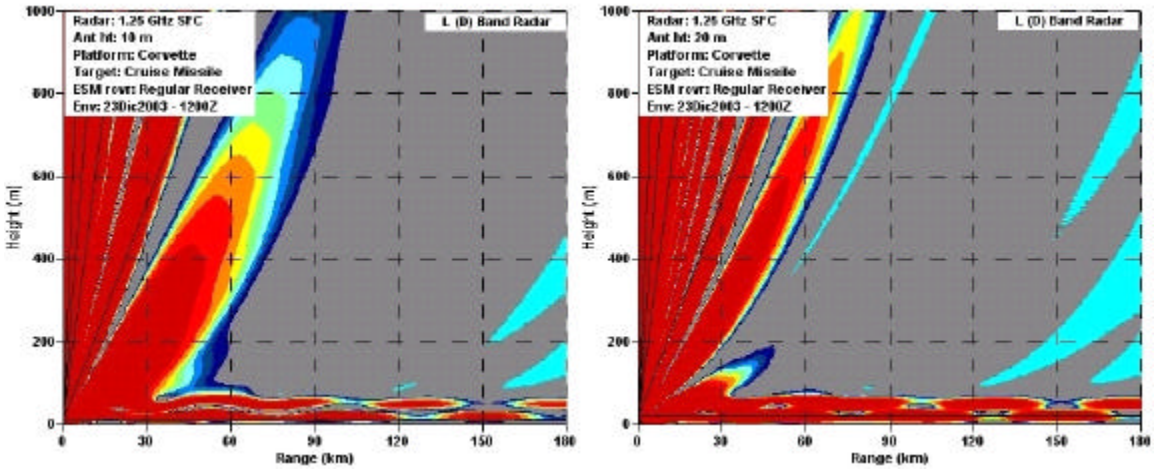

Figure 18. Propagation patterns for an L band radar on 23 December at 12Z, with antenna heights of 10, 15 and 20 m

As expected, the strongest effect was noticed when the height was 15 meters, that is, just below the top of the EVD (Z^*), which was strong enough to trap the lowest lobes of the radar pattern. Higher antenna positions (15 and 20 meters) appeared to prevent, to some degree, these detection reductions above the top of the duct, whereas the normal refraction pattern does not anyway allow a complete detection in the whole area.

On 24 December, one day before the front reached this area, the M gradients in the upper levels were severely reduced, as well as the heights for the top of EVD, with Z^* down to less than 7 meters as shown in the previous graph, with a superrefractive profile from the low levels all the way up to about 400 m, where there was in fact an elevated duct (Figure 18). The resulting propagation patterns are not very different from those of a standard atmosphere for the lower radar frequencies, other than surface detection ranges almost doubling (from 30 to 60 km) for the X band radar only, because of the thin EVD.

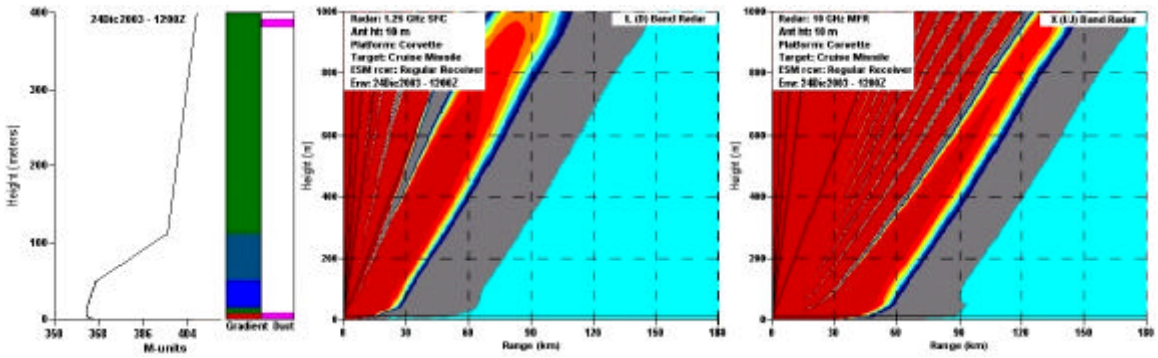

Figure 19. Refractivity profile for 24 December, at 12Z, and the resultant propagation patterns for L (center) and X (right) band radars

After the system passed early on 25 December, the enhanced low level mixing due to the strong winds associated with the front (Figure 19) appeared to reduce even more the Z^* for the following 48 hours, but also created a thick SBD (up to 110 m and 170 m on 25-26 December, respectively), with serious implications for the EM propagation profiles. On both days, the SBD was capable of trapping all the range of frequencies, producing again enhanced detection ranges in surface levels, while clearly reducing them above the duct.

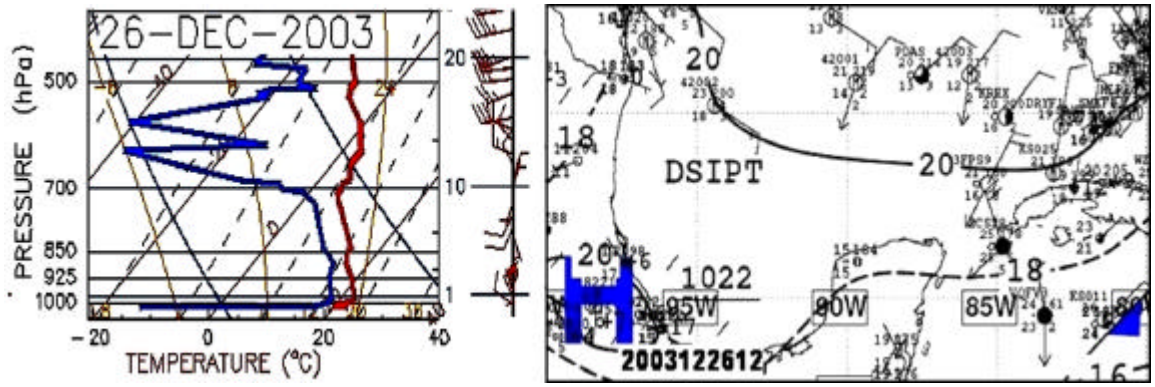

Figure 20. Surface Analysis (After NOAA FSL, 2004) and Skew T plot (After NOAA Tropical Prediction Center, 2004)for 26 December, at 12 Z, showing the conditions after the pass of the front cold

Since the evaporation duct was almost negligible, there was no evident difference between the offshore and the inland bearings of the antenna. The most remarkable effect was for the L and S bands, where the trapping SBD produced maximum detection ranges well beyond 200 km, but also several strong gaps without any detection at all at the surface and near the top of the duct. This should be a very important consideration for

operational purposes, since any low level target, such a low flying aircraft, small fast boats or sea skimming missiles would not be consistently tracked, or even worse, they can move along such areas completely undetected.

On 25 December, the X band achieved the best performance since the ray tracing results showed an almost uniform coverage along the surface, without severe gaps (Figure 20), although changing antenna heights did not make any difference.

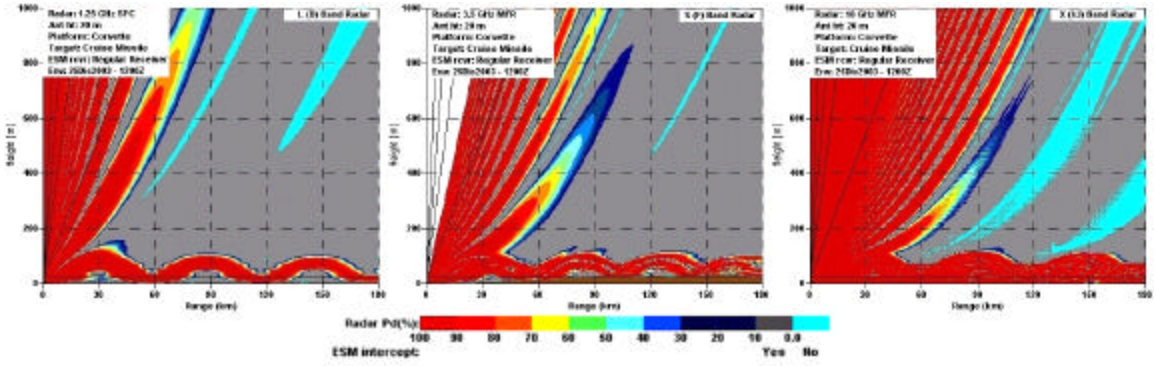

Figure 21. Propagation patterns on 25 December at 12 Z, for L,S and X band radars, with an 110 m thick SBD

The observed degradation was even more dramatic 24 hours later (Figure 21), when a thicker SBD (up to more than 170 m) combined with an extremely low Z^* (3.4 m) produced a very large single gap without detection capabilities from about 30 km or less, all the way to about 120-150 km, where the presence of a wide zone of strong detection may create a false feeling of confidence in the operators, if they are not aware of the existence of such blind zones.

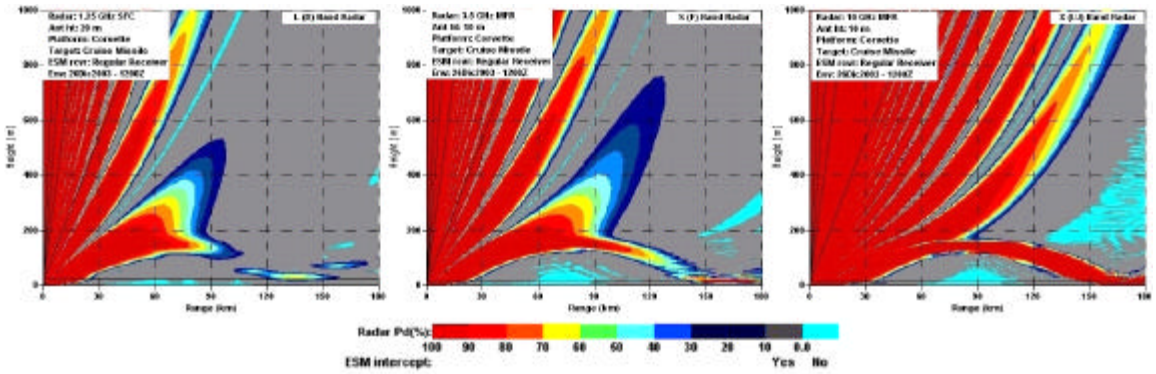

Figure 22. Propagation patterns on 25 December at 12 Z, for L,S and X band radars, with a SBD more than 170 m thick

Another important fact was that the evening surface data showed some recovering of the EVD thickness, with Z^* of about 12.7 m (very similar to the monthly "climatological" value), which would also yield a much lower SBD (25 m) when appending to the radiosonde profile. In other words, the propagation patterns just described would vanish in a matter of 12 hours, and only the X band radar could achieve enhanced detection ranges in the lower levels (Figure 22).

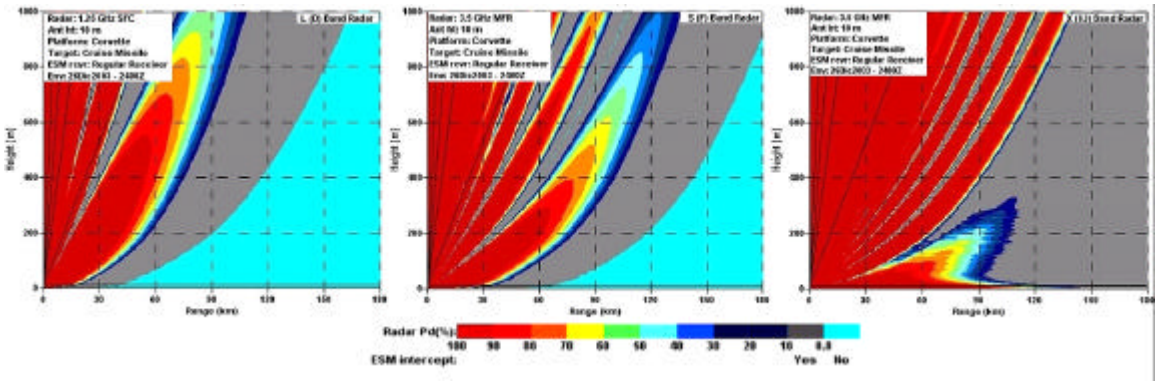

Figure 23. Propagation patterns for 26 December with 24Z surface data, for L, S and X band radars, when the SBD apparently vanished

Despite the fact that the evening profiles may not be valid for the upper levels because of the lack of radiosonde data at 24 Z (1800, Local Time), the surface data gave evidence of the variability in the Z^* values for the EVD. When the expected M gradients are not very strong, as in the case on 26 December (Figure 23), these can be very feasible results; hence the relevancy of better availability and resolution for both surface and upper air data when more reliable results are required.

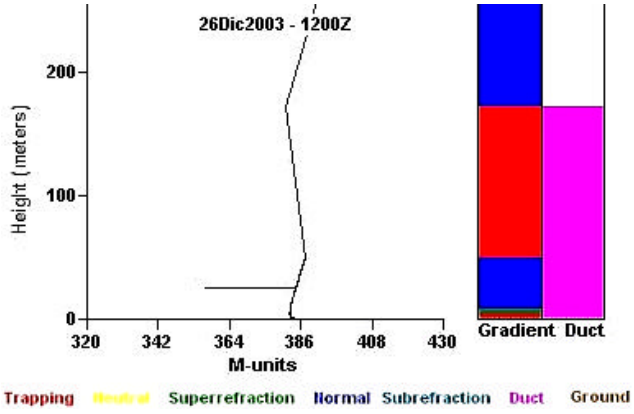

Figure 24. Refractivity profile for 26 December at 12 Z, showing a weak M gradient and Z^* after appending with radiosonde and surface data.

Finally, on 27 December, the thickness of the SBD was nearly 85 m, and the EVD grew back to a Z^* of about 18 m, a few meters above the usual heights for the radar antennas in a medium size corvette or patrol boat. This may normally be expected since the subsidence associated with the high pressure air mass behind the front should enhance the layering and the EVD, so the propagation patterns would also look much like those of 23 December, before the frontal system influenced the area (Figure 24).

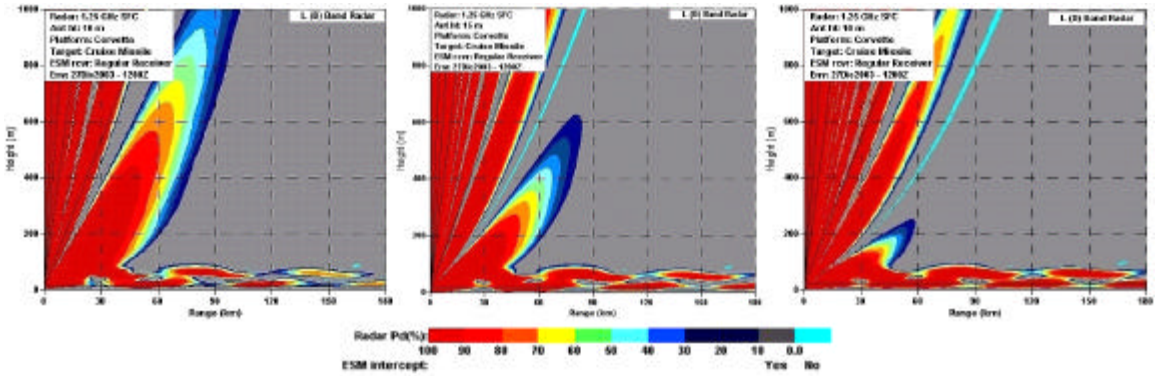

Figure 25. Propagation patterns for 27 December at 12 Z, antenna heights of 10, 15 and 20 m, SBD thickness of 85 m, and Z^* about 18 m

C. CASE STUDY 3: TROPICAL CYCLONE

During the tropical cyclone season, according to the AREPS statistics, there is an apparent coincidence between the higher probability of the occurrence of ducts, the enhanced diurnal variability of such occurrences during the summer, and the lowest climatological Air-Sea surface temperature differences.

For this scenario, the period from 9-14 July was analyzed because the Tropical Storm Claudette crossed the Yucatan Peninsula from the Caribbean Sea to the Gulf of Mexico, with its center reaching land only a few miles South of Cancun on 11 July, approximately at 12 Z.

Approximately 72 hours before the cyclone approached the area, the radiosonde data showed smooth profiles in the upper layers; one day later, there were evident low Z^* values of 6 to 10 meters (Figure 25), whereas the "normal" evaporation duct height based on monthly climatology data was 16 m, probably due to increasing winds and mixing ratios.

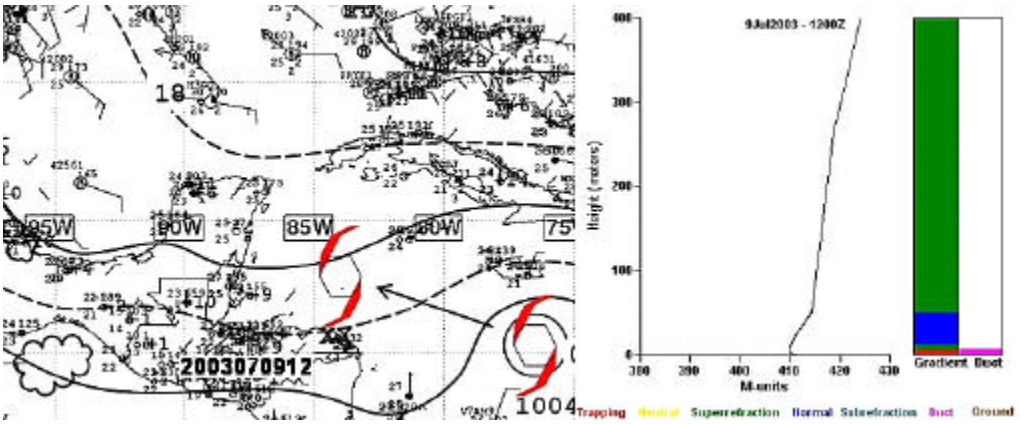

Figure 26. Surface Analysis (After NOAA Tropical Prediction Center, 2004) and refractivity M profile for 9 July at 12 Z, nearly 48 hours before the arrival of tropical storm Claudette

However, around 600 to 1,000 km away from the center of the cyclone, a significant superrefractive layer appeared from about 60 to more than 400 m. This was apparently due to the dry air subsidence associated with the outer shear line (Fujita and Tecson, 1973), which produced significantly extended detection ranges in those levels for all the frequency bands. At the surface, the EVD only affected the X band radar with some detection range enhancement, but no trapping was possible because of the low Z^*.

When the cyclone was between 300 and 500 km away from the area, 24 hours before landfall,, the M gradients were reduced, and a superrefractive appeared to build a thick SBD. The surface profile itself showed an apparent SBD with a top height of about 26 m, but after appending it to the upper profile, this height was increased up to almost 410 m (Figure 26).

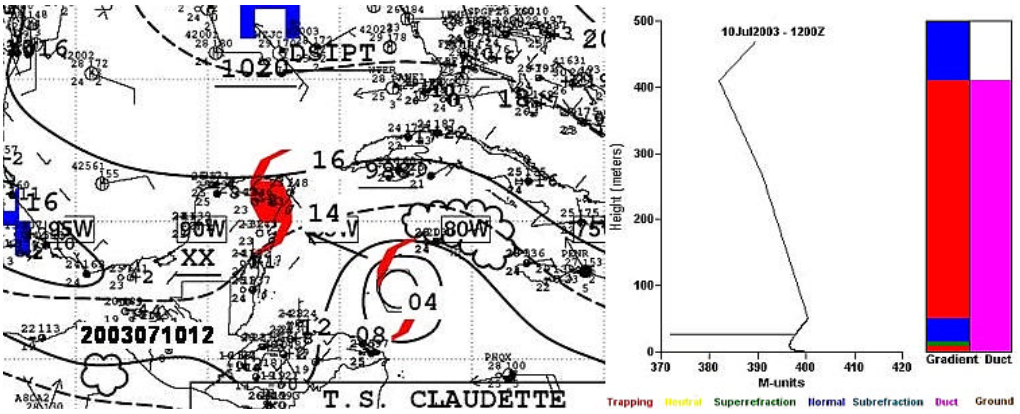

Figure 27. Surface Analysis and refractivity M profile for 10 July at 12 Z, 24 hours before the arrival of tropical storm Claudette

Again, the resulting SBD radically changed the operational environment for EM propagation in all the radar bands. The lower lobes were strongly refracted and trapped, creating an extended zone of surface detection ranging between 120 and 200 km, and a large gap with no detections at shorter ranges down to approximately 30 km, and in some cases less than that, depending on the radar band (Figure 27).

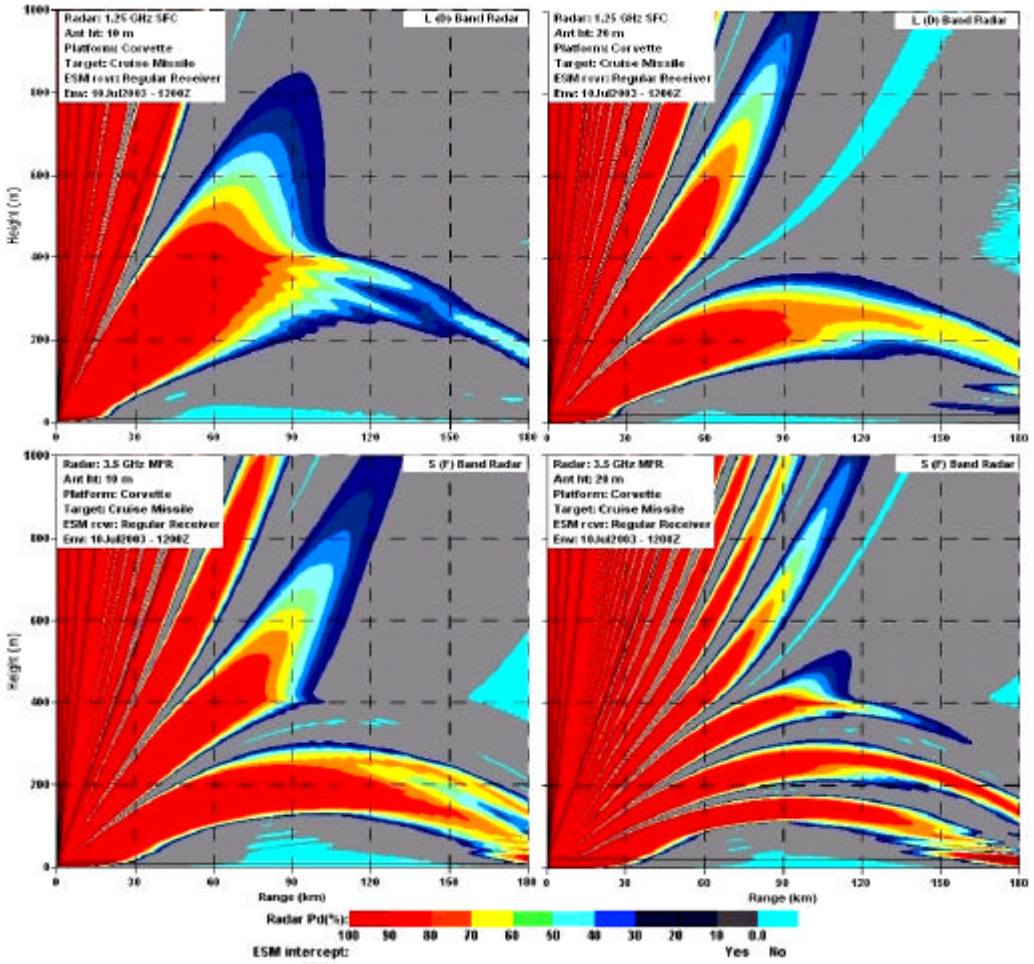

Figure 28. Propagation patterns on 10 July at 12 Z, with antenna heights of 10 and 20 m for L (left) and S (right) band radars

The antenna height proved to be a factor only for the L and S bands, while X band radar was clearly affected by the direction of the antenna offshore or inland (Figure 28), because of the differences in the computation of EVD profiles by AREPS, which was previously discussed. This was very important since the surface ranges were greatly increased up to approximately 90 km offshore, significantly reducing the gaps without detection otherwise created.

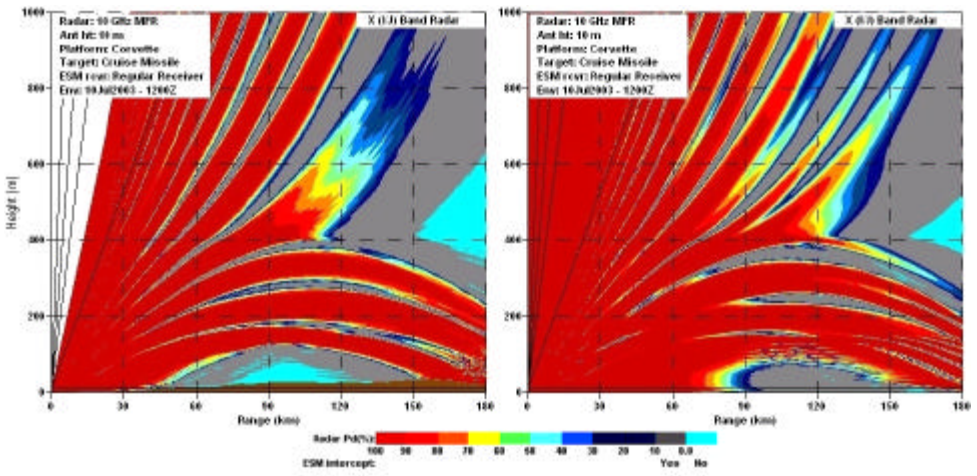

Figure 29. Differences in the propagation patterns on 10 July at 12 Z, for an X band radar with antenna height of 10 m, when scanning inland (left) and offshore (right)

At this time, the propagation patterns showed radical changes, so the upper air profile was appended to the evening surface data as an attempt to explore the effects of the changes in the lower level variables in shorter periods. Regardless of the "artificiality" of the SBD depicted with a 400 m top height, the surface data produced a thicker EVD with Z^* of almost 19 m, an increase of almost 10 m in 12 hours, being now strong enough to enhance the surface detection ranges for the S band radar as well. On the other hand, the antenna height was now an important factor for the X band radar, clearly increasing the detection range from about 40 to almost 90 km when it was raised from 10 to 20 m (Figure 29).

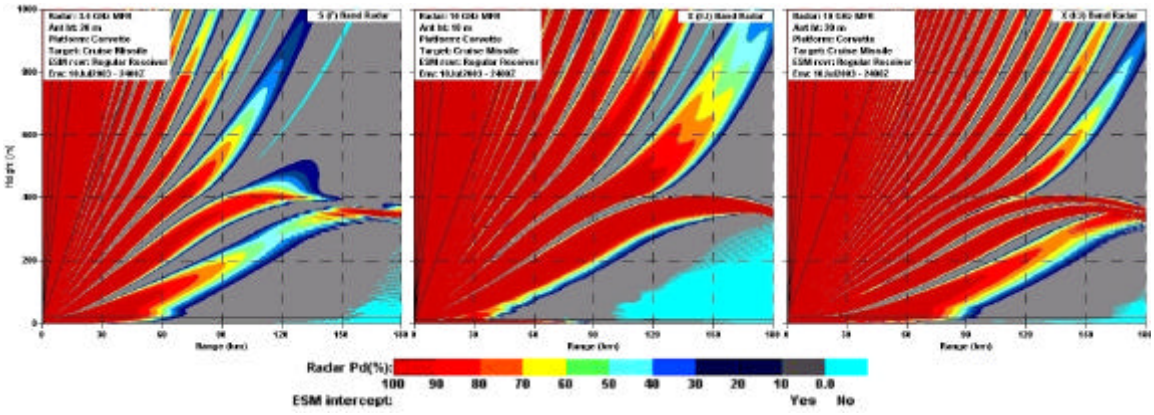

Figure 30. Propagation patterns for 10 July at 24 Z, for a S band radar at 20 m (left), and X band radar with antenna heights of 10 m (center) and 20 m (right), as tropical storm Claudette was approaching

The effects already discussed in previous paragraphs, seemed to be contrary to the expected results of reduced surface detection ranges when the antenna height was above *Z**. However, the radar horizon was effectively increased with the antenna height. Additionally, at least half the radiation beams of energy transmitted from the antenna (assumed to have a 0° elevation in all these scenarios) could be running almost parallel along or below the top of the EVD, since these values cannot be taken as hard limits.

On 11-12 July, as expected, high winds and strong mixing due to the storm produced very smooth profiles (Figure 30) without significant differences from the standard profiles, other than consistent evening increases of *Z** to about 17 m, with the resultant enhancement of the surface detection ranges for both S and X band radars.

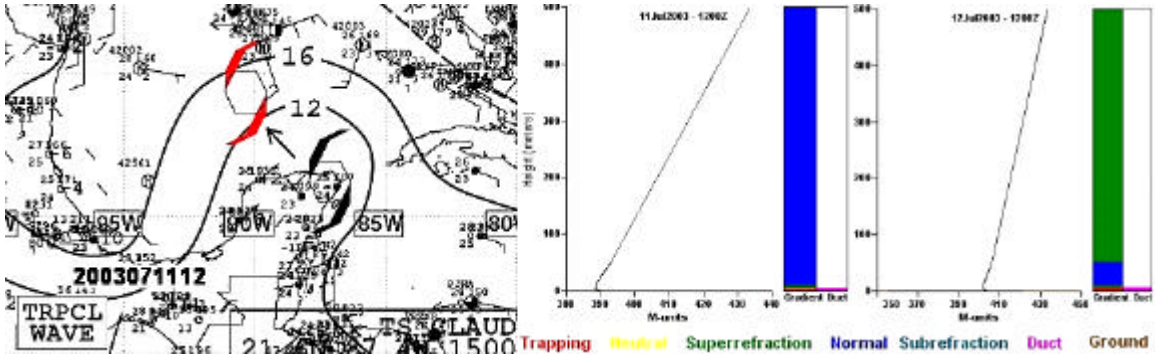

Figure 31. Surface Analysis (left) and refractivity M profile (center) for 11 July, nearly at T.S. Claudette landfall, and for 12 July, all at 12 Z

As the storm moved away, the evaporation ducts appeared to return to their normal values gradually, with the 12 Z profile showing a *Z** of 10.6 m on 13 July. This was thick enough to enhance the detection range clearly for the X band radar up to more than 100 km in surface, and to more than 120 km in the 400 m level. It was also clear that an antenna height of 20 m for the X band radar would neglect such an enhancement as expected, since the top of the EVD was now well below the antenna.

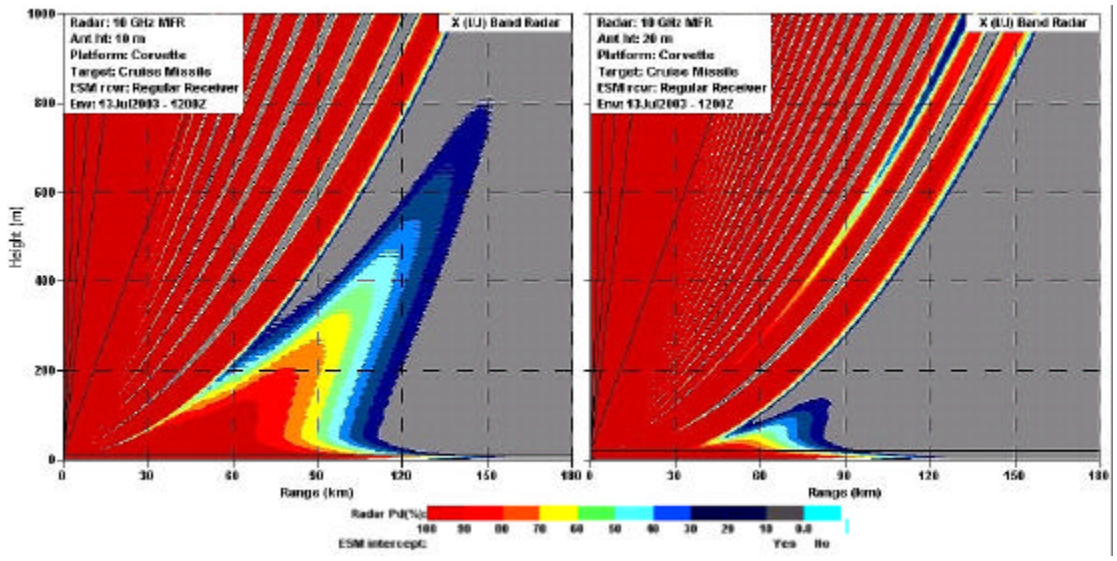

Figure 32. Propagation patterns on 13 July at 12 Z, for an X band radar with antenna heights of 10 and 20 m

Finally, on 14 July, the 12 Z profile (three days after the storm passed) was very similar to that of 10 July (Figure 31). Although the surface based duct did not appear, there was actually a thick elevated duct between 300 and 500 meters. Since the M gradient was not very strong, this can eventually be a realistic result.

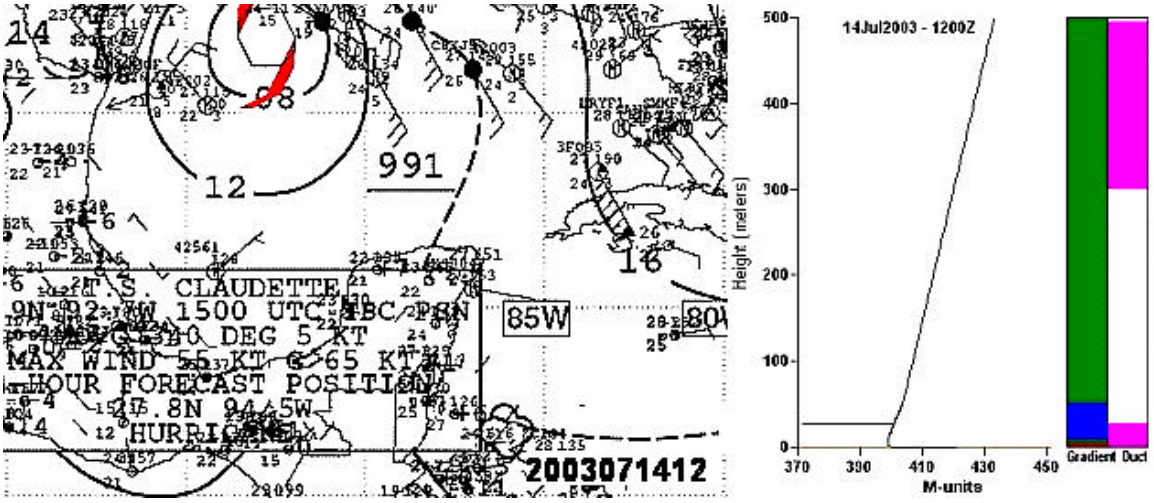

Figure 33. Surface analysis (After and refractivity for 14 July at 12Z, 48 hours after the tropical storm Claudette

AREPS may produce very different results when using the resulting refractivity profiles with different platforms and frequencies, and it is evident that the operationally implications will be very significant. As an example, a couple of days before the storm

approached, the lower evaporation ducts can make it very difficult to detect low surface targets. On the other hand, the radar capabilities for the Search and Rescue (SAR) of small boats and potential victims of the storm may be enhanced, in contrast with the Command and Control of the air assets usually employed (such as helicopters and low flying airplanes), which may be disrupted by the surface based ducts, depending on their relative positions and frequencies used.

THIS PAGE INTENTIONALLY LEFT BLANK

VI. THE USE OF IR SYSTEMS

The case studies in the previous chapter discussed how EW system performance can be modified by METOC factors, showing atmospheric refractivity to be particularly important for Radar and ESMs. EO/IR systems have been devised as a convenient option to overcome limiting factors with RF systems, particularly for passive detection and the tracking of potential targets. Regardless of their purpose and their inherent lack of range measurements, RF system major problems are clutter rejection and spectral band selection.

Different backgrounds such as terrain, cloud types and sea conditions, can severely degrade the detection capabilities against dim targets when low signal-to-clutter ratios are likely to occur. Further, depending on the spectral band selected to operate, different threats under extreme variations in the environment will result in different detection ranges and performances.

As a general rule of thumb, scattering by both molecules and aerosols is of greater importance in the visible, and even more so in the ultraviolet. On the other hand, absorption and scattering are equally important in the medium wave infrared (MWIR, 3-5 μm) while absorption is the dominant factor in the long wave infrared (LWIR, 8-14 μm). Thus, the problem appears when their performance must be assessed under critical operational conditions, which is usually a more difficult problem than it is for RF systems.

A. MEASURES OF PERFORMANCE FOR IR DEVICES

Despite the wide variety of designs, the analysis of EO/IR systems can be based on two main components, the internal hardware or components, and the external factors such as the transmission medium, background and other sources of noise.

The maximum achievable range is always a concern for EO/IR devices, and this can be calculated in several ways. For detection of a target with certain source radiant intensity I by a simple single IR detecting element, it can be expressed in a form of the range equation similar to that for radar. In this case, it accounts for a one-way propagation only, which is correct for passive systems. Although somewhat

oversimplified, the operational parameters of the whole system can be grouped together to give a good insight about the general approach for analysis of EO/IR systems (Cooper, 2003), yielding an equation in the form:

$$R_0 = [I\, t_a]^{1/2} \left[\frac{p/2\, D_0\, NA\, t_0}{\Omega^{1/2}}\right]^{1/2} [D^*]^{1/2} [(DT)\Delta n]^{-1/4} \tag{6.1}$$

In this equation, the achievable range R_o is the result of four main factors. The first factor accounts for the intensity of the source of radiation I and the propagation medium, expressed in this case by the transmittance t_a, or attenuation component of the atmosphere. The second group describes the characteristics of the optical receiver by its aperture diameter D_o, the relationship between this and the focal length (known as Numerical Aperture, NA), the instantaneous field of view Ω, and the overall transmission factor t_o of the receiving system itself, which includes the optical efficiency. The detecting element is globally expressed by its specific detectivity D^*, which is a function of the detector responsivity, its dimensions, and the electronic noise bandwidth. Finally, the fourth group involves signal processing, which in this case sets the threshold for detection when the voltage of the input signal equals the voltage of the system's noise, with respect to the electronic noise bandwidth. In other words, the resulting range R_o will be such that the signal-to-noise ratio has its threshold value SNRT so the target is just detectable.

However, defining the limit of detection by the signal-to-noise ratio is rarely used for modern EO/IR systems, since they are typically limited by contrast, not by sensitivity. Therefore, the SNRT criterion is usually replaced with a thermal contrast criterion (Minimum Resolvable Temperature Difference or equivalent).

Spatial resolution is the ability of an imaging system to distinguish separate objects or parts of an object within its field-of-view. Another measure of performance is the thermal resolution, or the smallest temperature difference a system can distinguish an incoming signal from the background noise in the system.

Sometimes thermal resolution is described by the noise-equivalent temperature difference NETD or the temperature variation that changes the collected flux by an amount equal to the noise-equivalent power NEP. Therefore, NETD gives insight into a

system's ability to detect small signals in noise, depending on several factors such as aperture diameter, sensor band average detectivity, the number of detectors, scan efficiency, FOV, and frame rate (Holst, 2003). On the contrary, NETD defines only the temporal detector noise, and not spatially. Therefore, it is normally used only as an intermediate sensitivity parameter for simplification of formulations of more specific performance parameters.

The most used specification parameter for FLIR systems is the Minimum Resolvable Temperature Difference MRTD, defined as the temperature difference between the background and a set of four standard bars required to make the bars just resolvable, as a function of their spatial frequency. Thus, as the bars become smaller, the required temperature difference to resolve them increases. This measure includes both resolution and sensitivity, and it is subjective since it involves the judgment of the human observer.

Similarly, Minimum Detectable Temperature Difference MDTD is the temperature difference between an isolated square and a uniform background that makes the square just detectable, as a function of its dimensions in spatial frequency. As in the case of MRTD, it also involves the subjectivity of an observer. The difference between them is the representation of the target, which for MDTD, is a square rather than a four-bar target (Goksin, 2000).

As a generalization, the thermal and spatial resolution may be considered inversely proportional, because the thermal resolution (or NETD) can be improved by increasing the size of the detecting elements, so more flux will be collected by each, but this would degrade the spatial resolution by increasing the IFOV. Therefore, neither is a good measure of the overall IR imaging system performance. The single quantity MRTD, which is determined experimentally, measures both performance factors simultaneously and takes into account all the various theoretical and real-world factors that matter.

The atmospheric transmittance t_a, which is the most limiting factor for EO/IR systems, strongly depends on the local meteorological conditions, as well as on the geometry and length of the range path. In a practical approximation, t_a is written as a simple exponential function of the atmospheric extinction coefficient m in the form $t_a = e^{-mR}$, such that:

$$R_o = R\left[t_a\right]^{1/2} = Re^{-mR_o/2} \tag{6.2}$$

where R is the maximum range with no atmospheric attenuation. Note that the solution R_o, appears on both sides of the equation, so it cannot be solved in closed form, but it can be numerically evaluated by several methods, by writing

$$R_{left} = R \text{, and } R_{right} = Re^{-mR_o/2} \tag{6.3}$$

Then, the simplified equation may be solved graphically by plotting both expressions as functions of the general range R. The intersection of the two curves gives the maximum achievable range R_o under these conditions (also given by $R_{left} - R_{right} = 0$). The graphical solution displayed in Figure 33 is an example of a "typical" set of parameters, with attenuation coefficient 0.2/km. In this case, the maximum computed range R is 32.36 km when the atmospheric attenuation is neglected $m = 0$, so the starting point for R_{right} is $R = 0$. The maximum range for detection is $R_o = 10.8$ km, which shows that even a moderate level of attenuation can severely degrade the detection range, in this case, to almost one third (Cooper, 2003).

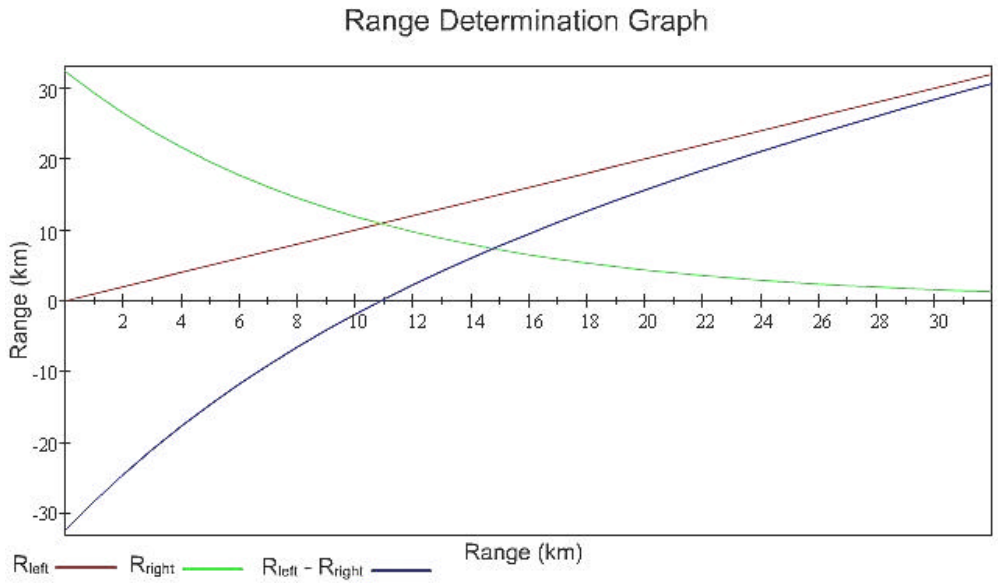

Figure 34. Graphical solution for the maximum achievable range for a generic IR system, when $m = 0.2/\text{km}$

The range equation can then be solved to evaluate the effectiveness of a specific design, or the feasible trade-offs when the design is changed, for example to minimize costs or to fit the system geometry to a required platform, while maintaining the required detection range.

Although very convenient, this simple model has some major defects, since the target signature I (given in W/Sr) must be replaced with a function of wavelength over the optical bandwidth of the sensor. Similarly, the atmospheric transmittance must be averaged over the optical bandwidth of the sensor system along the optical path, while also related to the meteorological conditions, since the attenuation coefficient is largely dependent on wavelength, temperature and pressure, relative and absolute humidity, and atmosphere composition. Even further, not all the radiation reaching the detector comes from the emitting source outside the scene, since the atmospheric path itself can also act as a source of radiance. In practice, this evaluation can only be done using the appropriate computer codes such as MODTRAN or LOWTRAN.

IRST systems design often regards the achievable probability of detection P_d in a single scan or frame, given a maximum tolerable false-alarm rate FAR and making several assumptions such as a specific target, background, environment, and weather.

This is useful because P_d is determined by the threshold of signal-to-noise ratio SNRT, while the FAR is defined by the system's noise level (Accetta and Shumaker, 2001).

B. PROPAGATION ISSUES FOR EO/IR WAVES

It is clear that effective predictions of performances are critical to obtain the best solution, but despite the technical improvements in IR sensor technologies, the complexity of the environmental limiting factors makes such predictions much more difficult than for RF systems.

The atmosphere is not a purely transparent medium since molecules and larger particles in the atmosphere attenuate the propagating radiation, while background radiance (solar and thermal) may completely mask IR targets. To predict the performance of EO/IR systems effectively, three major atmospheric factors affecting the propagation of an optical energy must be assessed, as well as their fluctuations. Those are refraction, extinction (by absorption and scattering), and turbulence.

Refraction is the bending of light rays due to refractive index gradients in the atmosphere, which was analyzed in detail for the case of RF systems. In the optical spectra, it is evident by the presence of mirages. However, in the limited ranges of EO/IR systems, this is not usually a significant problem, except for laser illuminators and target designators.

Turbulence are small scale inhomogeneities of the index of refraction creating distortions of an optical beam (such as beam wander and broadening, and scintillation*)*. They are not significant in propagation of longer EM waves, yet their size is comparable to the optical wavelengths, so they are very important in propagation of the shorter IR waves. As a result, the resultant image can be blurred, distorted, or changed only from scene to scene, depending on the relation between the integration time in the detector elements and the scale of the turbulence.

For turbulence, temperature is the most important factor. Therefore, it can exhibit strong diurnal cycling, and is distinctively influenced by the presence of sources of convection along the atmospheric path. As a consequence, the usual tactical prediction methods do not account for turbulence effects, particularly for distortion in imaging devices, yet significant improvements have been made to predict laser beam spreading,

since it is a critical issue for target illuminating systems and range finders. The prediction of turbulence requires precise estimations in time and space of the atmospheric pressure temperature, relative humidity and wind speed at the sea surface. This problem can be simplified by using the bulk method, given that suitable values of such variables can be obtained at some reference height (Davidson, 2003, p. 6-16).

Extinction is the attenuation or loss of energy of electromagnetic radiation. The attenuation of monochromatic radiation (except at very high flux density) can be described by a form of Beer's Law, also known as Bouguer's or Lambert's Law:

$$I(R) = Ie^{-\mathrm{m}R} \tag{6.4}$$

where *I(R)* is the attenuated radiation, *I* is the incident radiation, and *R* is the distance of travel or path length. The exponential factor e^{-mR} is also known as transmittance t since it is used as a coefficient to account for the fraction of radiance effectively transmitted through the propagation path as the ratio *I(z)/I*.

The attenuation coefficient m includes both the absorption and scattering effects of the atmospheric gas molecules m_a and of the aerosol particles m_b. The total attenuation coefficient is the combined effect of molecular absorption k_m, mostly from water vapor and ozone, molecular scattering s_m, aerosol absorption k_a, where absorption by dry particles is usually neglected, and aerosol scattering s_a, expressed by the sum

$$m = m_a + m_s = (k_m + k_a) + (s_m + s_a) \tag{6.5}$$

In theory, the transmittance for a given band can be exactly computed, given there is enough data available for density, temperature and pressure of all the atmospheric components, as well as their spectral response for each wavelength within that band. Since it is very difficult to evaluate it for each spectral line (wavelength), certain profiles of pressure, temperature and molecular densities for a waveband may be assumed.

Even in a low-resolution calculation for a standard atmosphere, the transmission spectrum is complex, as shown in Figure 34. It shows several regions of almost null transmission due to atmospheric propagation, where the 3-5 and 8-12 μm regions appear to be the most suitable wavelengths.

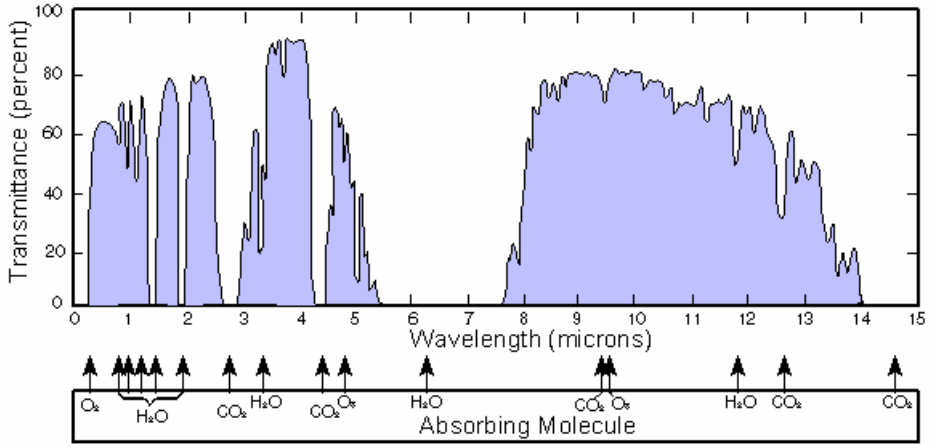

Figure 35. Typical transmittance of atmosphere for the IR region, over a 1 nmi path at sea level (From NAWCWPNS, 1997).

However, even between these two "windows," the performances of IR sensors may be significantly different. Generally, the 3-5 μm region has better transmission values, while the absorption extinction is more variable for the 8-12 μm over normal absolute humidity ranges. Thus, absorption can be a more degrading factor for the latter. Since water vapor is a major absorption parameter, shorter IR band systems could be considered more convenient for a low latitude marine environments due to the larger amounts of water vapor normally associated with such environments.

Scattering can be described by the relationship of the aerosol particle radius r versus the wavelength l of the incident energy, but the extinction coefficients for scattering are mainly determined from all aerosols with a certain distribution of sizes (Figure 35).

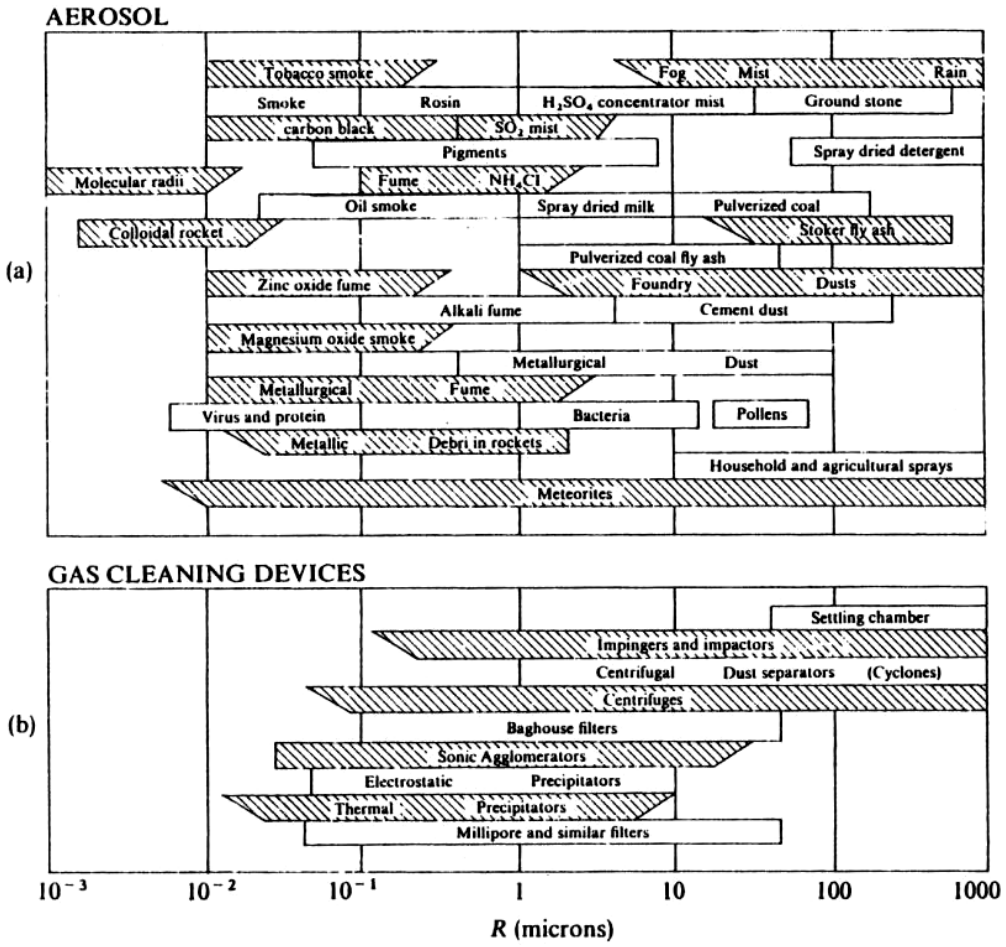

Figure 36. Classes and Sizes of Aerosols. (From Williamson, 1973).

The usual atmospheric aerosols in optical scattering are too small (with radii between about 0.1 and 1.0) for rain alone to reduce haze and increase visibility. Instead, radical changes in the vertical temperature profile (such as a frontal passage) do increase horizontal visibility through the increased upward diffusion of the aerosols (Davidson, 2003, p. 7-14). Scattering is also indirectly a function of relative humidity because when moisture increases, water molecules can accumulate on dry particles, making them grow quickly by deliquescence, creating rapid changes in the size distribution of hygroscopic aerosols and enhancing scattering.

Wind is clearly another major factor in aerosol distributions over the ocean, because it enhances the generation of salt particles at the surface, particularly in speeds between 5 and 8 m/s, normally associated with the formation of white caps. As a consequence, extinction can be expected to increase with the wind speed for all

wavelengths, yet shorter wavelengths are the most affected. It is important to note that in the area of interest, these wind speed are very similar to the annual climatological average of 6 m/s (GMCA, 2004).

Maritime environments are usually associated with natural large size aerosol backgrounds, being those more important degrading factors for the visible and near IR (3-5 μm) systems. As a consequence, when used in littoral environments, they may be more degraded than they would be on a continental area or than in the LWIR (8-12) systems.

C. THE USE OF MODELS AND TDAS

It has been shown that for the proper design and operation of IR devices, it is critical to predict the transmittance of the atmosphere as a function of wavelength and weather conditions. Such prediction is a complex problem of computer modeling, but fortunately, extensive efforts in the development of models, computer codes and voluminous data libraries have been made. They can be classified in three major groups, according to their function: target models, sensor models, and propagation models.

Target models are used to calculate the strength of the electro-optical signal at zero range for specific targets and background characteristics. They determine the radiance difference between the inherent signal emanating from the target and background, and converts it to an equivalent blackbody temperature difference via a thermal model based on three-dimensional heat transfer within the target as well as with the environment into a temperature difference ΔT at zero range. The target mean temperature and total projected area are used to compute range.

Sensor Models describe the sensor performance in terms of MRTD or MDTD as a function of spatial frequency. These models determine the detection or the lock-on range of an electro-optical system when applied to the apparent target signature.

Atmospheric Propagation Models to calculate the apparent temperature difference at the entrance aperture of the sensor by estimating the degradation of signal due to the atmosphere, such as LOWTRAN (Low Spectral Resolution Transmission), and MODTRAN (Moderate Spectral Resolution Transmission), have been more recently developed.

1. LOWTRAN (AFGL)

As previously explained, real sensor systems require propagation predictions for a relatively broad bandwidth, but satisfactory results can be analytically calculated in the band of interest by calculating average transmittances contributing to the instrument sensitivity ("band models") rather than characterizing numerous individual spectral lines.

Such an approach is used in the atmospheric model LOWTRAN (Low Resolution Transmittance) for fast computational capability with reasonably accurate results in the spectral region from ultraviolet to the far infrared. This makes it suitable for operational purposes at surface levels and the lower atmosphere, being seriously degraded for levels above of approximately 40 km.

IR transmission losses and sky backgrounds can be predicted using pressure, temperature and relative humidity (vapor pressure) from radiosonde data, and even from climatological profiles. In the meantime, they are largely determined by the effects of water vapor absorption along the path, and LOWTRAN can adequately account for them. However, non-representativeness of the profiles, the target parameters or the assumed aerosol distributions, depending on the actual environment, could lead to a considerable underestimation of scatter effects, with significant losses in accuracy.

Since aerosol absorption and scattering are required to describe total transmittance, LOWTRAN includes selectable aerosol size distribution models for continental and marine regimes, such as the Navy Aerosol Model (NAM) and the Naval Oceanic Vertical Aerosol Model (NOVAM).

2. Navy Aerosol Model (NAM)

Marine aerosol size distributions are different that continental, so in the littorals, mixed continental-marine aerosol distribution may be complex. The simple Junge exponential distribution commonly used in the past (Davidson, 2003, p. 7-13) cannot describe such a wide range in sizes of common aerosols. Thus, more realistic estimates of aerosol distributions are needed. The present version of the Navy Aerosol Model (NAM) represents the size distributions of the aerosols in the surface layer over the sea in terms of four lognormal components.

Three are determined by routinely measured and analyzed meteorological parameters. The fourth, the air-mass type parameter (AMP), is a number describing the general condition from a pure air mass without contaminants to the situation downwind of a large industrial complex in a corresponding scale from one through ten. It is not routinely measured, so it can be based on empirical judgment.

D. USING "TAWS"

The Target Acquisition Weapons Software (TAWS) predicts the performance of electro-optical weapon and navigation systems. It replaces the Electro-Optical Tactical Decision Aid (EOTDA) and the Night Vision Goggles Operations Weapons Software (NOWS) for mission planning decisions, to modify mission execution tactics or weapons usage, or to evaluate the general environmental conditions for Infrared (3-5 5 μm and 8-12 5 μm), Visible (0.4-0.9 5 μm, which includes both TV and NVG systems), and Laser (1.06 5 μm) systems already defined in its libraries.

TAWS was designed to predict the performance of air-to-ground EO sensors and navigation systems. If the desired sensor system is not included in its inventory, new IR, TV, NVG, or 1.06 5 μm laser sensors can be added, by manually defining the required characteristics. Since the data to input has too many options available, this may not be an easy task.

The types of missions supported by TAWS include target acquisition/detection, target designation and tracking, close air support, helicopter, refueling, take-off and landing, identification of pickup/drop zones, training, and search and rescue. A single mission may include several of these tasks.

Illumination Analysis computes solar and lunar positions, illumination and event times for a specified location. Point-Based Analysis calculates detailed performance predictions for several locations in a given area or locations along a mission route. It involves the computation of detection range, detection probability, or lock-on range for a particular target at a particular location under specified weather conditions. Map-Based Analysis allows such predictions for several targets in a complete Area of Regard (AOR).

TAWS can also use elevation data to improve target masking and target shadowing computations from the Topographic Engineering Center (TEC), Digital Terrain Elevation Data (DTED), or choose not to use any (Lake, 2003).

Some other interesting features allow determining the best attack axis for the specific time and altitude by combining the greatest detection and lock-on ranges, as well as the best time of day to attack a target or when the target detection surpasses a designated threshold of detection. The latter is also known as thermal crossover, since the sensor sees the target and the background as the same temperature, which is when there is no apparent thermal contrast and the target will be "invisible" to the system.

For performance prediction, TAWS uses weather, sensor, and mission information. Weather information includes humidity, temperature, wind, and aerosol analyses valid at the TAWS valid time as well as for the preceding six hours. These parameters are for surface weather data, surface layer information, cloud information and upper layer parameters, up to a 30-hour period of time (18 hours before and 12 hours after the time over the target TOT). This is a requirement only for IR sensors, because the target and background signature models need hourly data for a minimum of six hours prior to TOT, to account for the effects of time of day and weather (Pagitt and Brooks, 1993, 2003).

The user can input weather data manually or automatically download weather data, from either the Air Force Weather Agency (AFWA) or the U.S. Navy's Tactical Environmental Data Server (TEDS), but the user must have valid ID and passwords as well as access to the Internet. In this study, the input data was manually entered.

TAWS was used for demonstration only, to compare the effects on the variation of some basic parameters when enough data are available. TAWS attempts to derive information from what is available when data are not available for a particular location and time window, nor all the requested parameters, for instance, missing reports on cloudiness. If it is not possible, static default values are used. Therefore, serious limitations and cumbersome outputs may arise from not having properly defined surface and upper layer atmosphere information. The examples used show the relevancy in the proper definition of such data for the region of interest.

Since main interest is in comparing the influence of the atmosphere on similar detectors rather than engineering or design issues, available sensors from the TAWS libraries were initially chosen. Although TAWS and the included applications are not classified, the documentation that relates the characteristics of the sensors and their names is, the most common ones were selected from the original libraries and then customized. To achieve similar ranges (approximately 10-15 kms) on the MWIR and LWIR main wavebands, the MRT, MDTD, spatial frequencies and FOVs of the selected sensors were modified to be the same.

Narrow FOVs were used to achieve the longest possible ranges, assuming prior cueing to the sensor from any other system, otherwise, detection alone will be sensibly shorter in range. This left the operating waveband the only relevant difference in hardware between them, so the expected performance would be solely the result of the environment influences and the correspondent response of the sensors to them. Some basic parameters of these two sensors are specified in Table 5.

Sensor	**WAVEBAND**	Spatial frequency	MRTD (°K)	MDTD (°K)
		0.375	0.004	0.008
8510 (MWIR)	3-5 µm	0.750	0.010	0.018
		1.500	0.029	0.045
1510 (LWIR)	8-12 µm	2.280	0.074	0.083
		3.750	0.662	0.240
FOV (mrad)	0.25 x 0.25	4.500	2.262	0.370
		5.250	13.30	0.637
		6.00	92.80	1.102

Table 5. Characteristics of a generic IR sensor, used for demonstrative purposes of an operational evaluation of performance

As it turns out, none of the sensors already available in TAWS could achieve more than 15 km under the actual conditions used. This result is also in agreement with the most evident limitation for the IR sensors of the reduced line-of-sight (or equivalently

the slant range), which in this scenario resulted to be about 13 km with a height of the sensor of 15 m, as shown in Figure 36. Increasing the heights should produce extended ranges only for more capable devices, which are not commonly available.

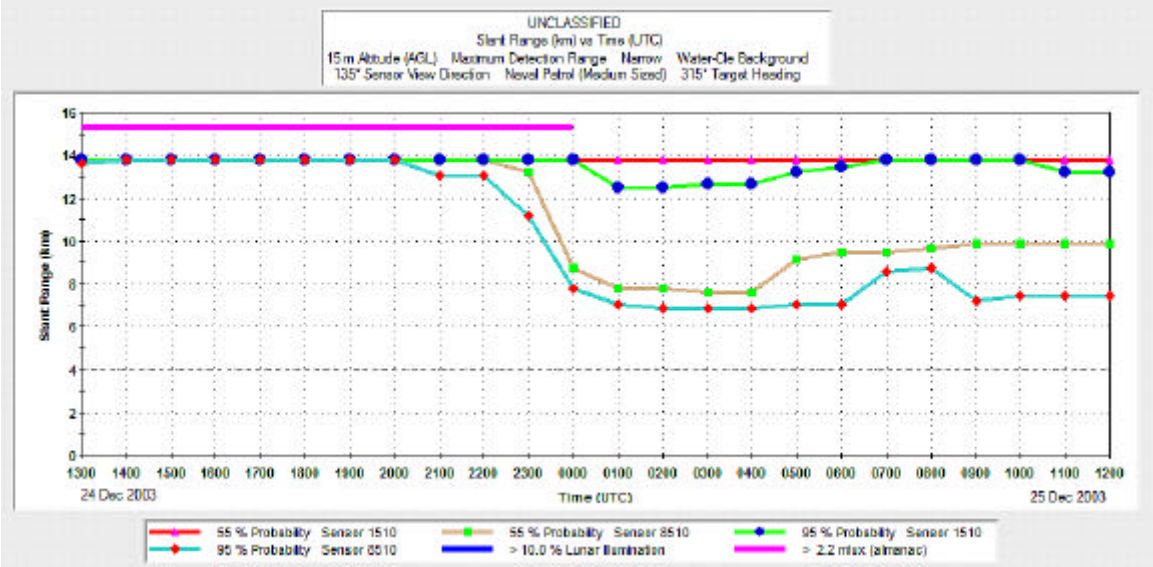

Figure 37. Hourly variations of achievable slant range for sensors 1510 (LWIR, 8-12 mm) and 8510 (MWIR, 3-5 mm) for 24-25 December

The first example was based on the available data for 23-25 December, when the passage of a front cold was proven to modify limit the radar performance to ranges less than 30 km (almost 15 nmi). Initially, the analysis of Slant Range versus Azimuth Angles clearly showed the differences between the two sensors, as well as the direct influence of the azimuth. This particular case shows the results after sunset (25 December at 00 Z), with the moon already enhancing the detection when the target (heading to 315°) is seen from the southwest (sensor heading to 060°). Interestingly, the LWIR performed sensibly better than the MWIR with longer ranges roughly by ½, as shown in Figure 37, because the latter was remarkably sensible to the AMP number and to the humidity changes. In all cases, the MWIR was also severely degraded after sunset, while the LWIR sensor was not very affected.

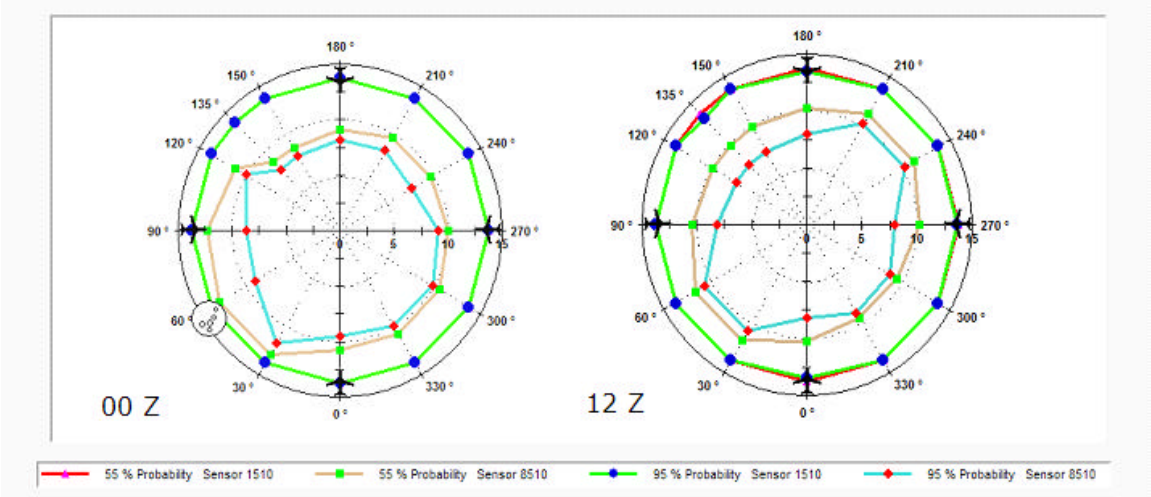

Figure 38. Plot of achievable slant range versus azimuth of the sensors for 25 December at 00 Z (left) and 12 Z (right)

These plots are useful to provide insights about surveillance direction distribution. TAWS can only display two dimensional graphs of the range performances. However, even when they show significant differences within only 12 hours of separation they do not show the variability of the atmospheric factors clearly. This is better displayed in time series of P_d (in these examples, displaying 24-hours periods), given the maximum ranges of 11 and 13 km. These plots start in 24 December at 1300 Z, finishing in 27 December at 12 Z (Figure 38), which show the effects of the weather associated to the pass of the cold front.

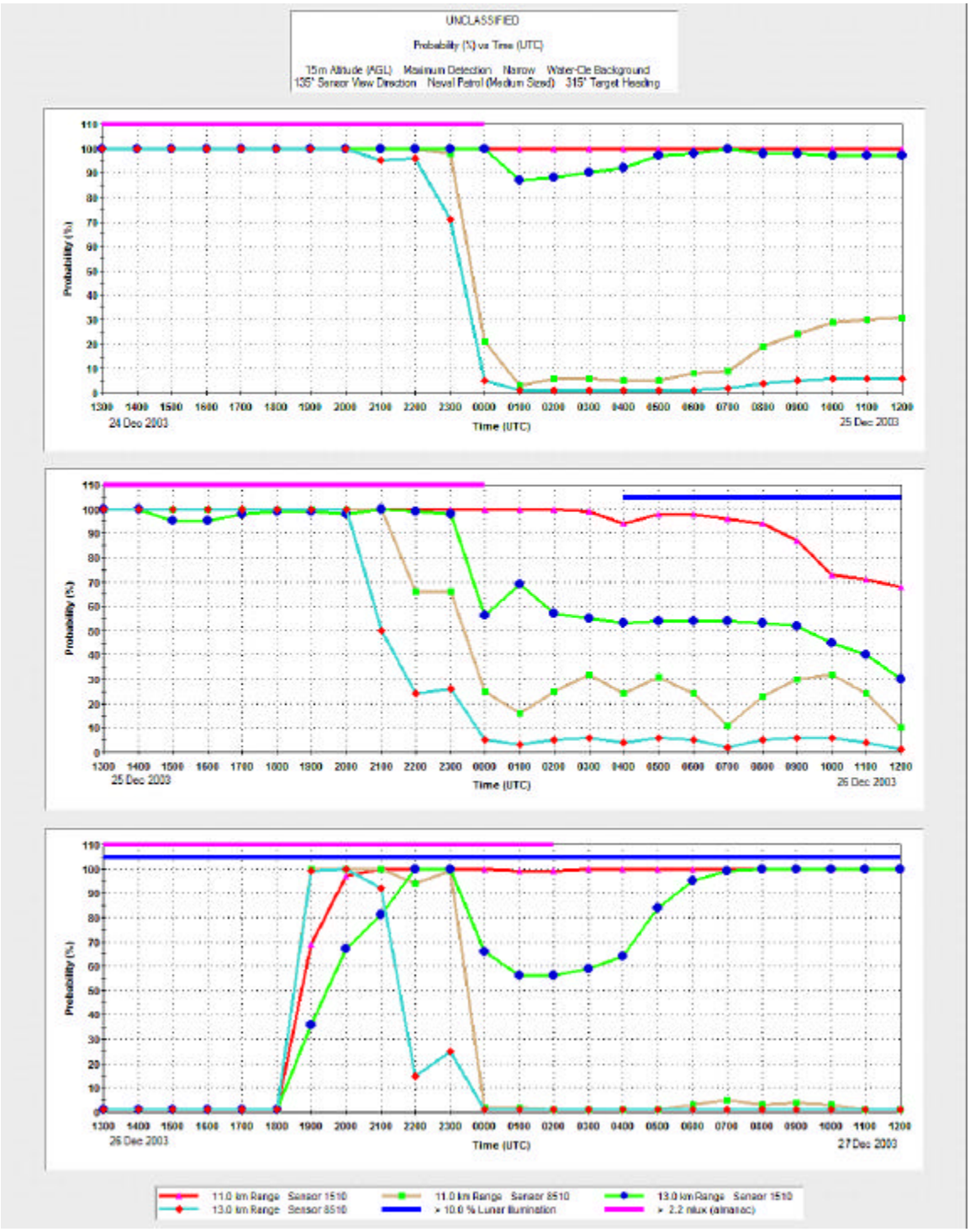

Figure 39. Hourly variations of achievable P_d for 24-25 (top), 25-26 (middle) and 26-27 December (bottom), showing the effects of a cold front.

It is important to note that the conditions depicted in the first series do not match the following one in the bottom panel, which transition is at 25 December, 1200Z. The

former shows an important degradation of detecting capabilities after a 24 hours period under influence of the weather (right at the expected arrival of the front, end of the upper panel). It does not exactly coincide with the depiction in the second panel, which includes data only from the previous six hours (0700 through 1300). This is important to note that for TAWS, IR sensors do need weather inputs for times prior to Time Over Target (TOT), thus the lower panel does not show the severe degradations for the MWIR sensor (Id. 8510), which in this case would be a tremendous difference, misleading the predictions of expected P_d.

Another evident and important result is shown early in December 26, 1100 through 1800, where rain (particularly heavy at 1500 Z) completely prevented the detection with IR sensors. Just after the rain, the MWIR sensor (Id. 8510) performed even better than the other, presumably because of the combination of gales and rain momentarily cleared the atmosphere. However, as the wind persistently intensified, the MWIR was severely degraded very rapidly, and even the LWIR sensor showed some affectation, which can be clearly related to the increase in aerosols distribution.

A second example was based upon the extreme case of tropical storm Claudette, which impacted the area of study in the morning of 11 July. The extreme weather conditions associated, and the relevance of high efficiency of operations along and after the passage of the storm, demands a thorough awareness of the achievable performance of the surveillance and detection systems.

The first evidence of atmospheric influences is the reduced performance in the evenings, this time even for the LWIR sensor, compared to what was achieved in the previous examples. This is an expected result after the increased temperatures (both atmospheric and sea surface), as well as the more humid environment. Similarly, the rain was clearly a strong limiting factor, which in this case will be very severe. Another significant result is that now the performance of both sensors was not that dissimilar, yet the MWIR sensor appeared to be much better near midday, degrading by the afternoon, when the LWIR sensor would be a better option.

More importantly, the approach of the storm proved to be a very range degrading event associated with moderate to heavy rain, as early as 10 July in the afternoon. This basically nullified both sensors until the afternoon of 11 July, when rain stopped and moderate winds cleared the atmosphere. It must be mentioned that the winds after the pass of the storm were also persistent and strong enough to increase again the number of aerosols in the atmosphere, but that happened in the evening; since the performance of both sensors for this seasons was normally reduced in those hours, the effect of such winds could not be clearly assessed.

Finally, after 12 and 13 July, when the effects of the storm vanished, the general performance of both sensors could be considered very similar again, with a strong response to the diurnal changes in temperature and humidity.

(a)

(b)

(c)

(d)

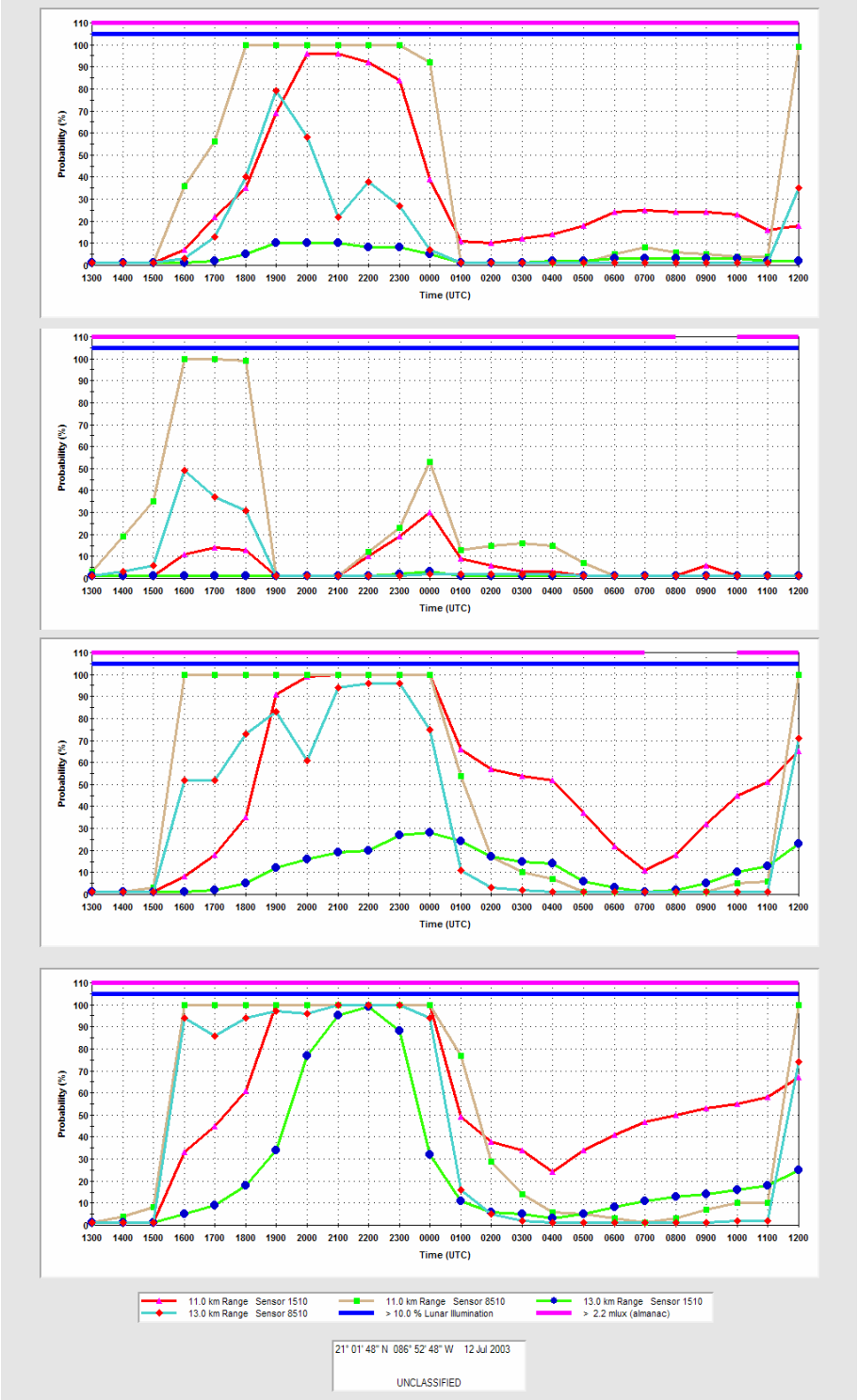

Figure 40. Hourly variations of achievable Pd for 8-9 (a), 9-10 (b), 10-11 (c) and 11-12 (d) July showing the effects of tropical storm Claudette.

VII. CONCLUSIONS AND RECOMMENDATIONS

A. GENERAL REMARKS

This work focused on the relevance of METOC factors on EM/EI system performances in tropical littoral environments. Tropical littoral regions are characterized by high water vapor content in the air above the surface, high probability of layering with anomalous electromagnetic propagation conditions, and the proximity to land influences. These factors can severely modify EM system performances and effectiveness, impacting on the typical operational scenarios of littoral warfare.

Under such conditions, the proper employment of EW systems, including short to medium range radars with higher resolution, and EO/IR systems for the proper implementation of EA and EP actions, planning, and conduct of future operations strongly depend on adequate evaluation and prediction of their respective performances with METOC factors included.

Technology improvements in the design of EW systems still encounter a major problem in atmospheric propagation effects that is very difficult to resolve. It has become very difficult to account for terrain features and atmospheric refraction, so the implementation of propagation models in computer based TDAs were proven to be a convenient solution.

Operational TDAs such as AREPS to analyze performances of both ES and radar systems are quite suitable since they work basically in the same RF bands. On the other hand, EO/IR systems are quite sensitive to a larger number of factors. Thus, the use of TDAs as TAWS is more complex, requires more and better data sources, and more training to use.

The evaluations of this study were made under the assumption of horizontal homogeneity of the atmosphere, which is seldom true. Hence high resolution data for the computer assisted TDAs to predict refractivity conditions are needed. The usual assumption of independence of the azimuth direction cannot suffice in littoral warfare, since the area of influence extends beyond the shore line and includes strong local effects

(such as orographic influences and coastal breezes). In that respect, AREPS, which allows for range dependence refractivity structure seemed to reasonably account for terrain effects along the path of propagation.

Similarly, statistics of tropospheric ducts showed evidently seasonal and diurnal signals, although in this study the only included data were from the radiosonde station of Merida, Mexico, and accounts for SBDs, but not but not for the overwater EVD.

A separate analysis was done with data from the GMCA to build what may be considered a "normal" monthly climatological surface profile. These profiles were built assuming that surface data itself allows the NPS model to describe the bottom of the boundary layer along the whole path properly. This is obviously a crucial but necessary assumption since there was not enough data to describe that path on its entirety effectively.

B. SUMMARY OF RESULTS

The resulting profiles showed EVDs with average height values (Z^*) very likely to impact frequencies above 4 and 8 GHz, respectively.

1. Seasonal and Diurnal Effects

The monthly climatological profiles demonstrated evident relationships between the Z^* values, SST and the air-sea temperature differences, although many other local factors and synoptic features are also expected to play a major role in the expected variability of the propagation characteristics.

The influence of diurnal variations in temperature, humidity, pressure and coastal breezes were usually strong enough to clearly modify the regular EM propagation, yet their interaction with major synoptic and mesoscale events and their associated weather resulted in very complex patterns, which are not easily predictable.

2. Winter and Cold Fronts

Particularly important for considering EM/EO sensor operational purposes were the highly predictable cold fronts, repeatedly appearing in the area with only a few days of separation, during specific seasons, to produce significant anomalies in the refractive conditions in a matter of only a few hours, dynamics and instability patterns just ahead of

the front line, as well as strong subsidence, normally exist in the adjacent areas behind the front, as well as other atmospheric features such as cloudiness, fog, or rain, which severely modify the performance of EW systems.

The frontal passages caused disruption in the local profiles. This caused radiosonde data available every 24 hours to be not good enough to depict such profiles in detail. A better understanding of their effects would be highly beneficial to optimize the performance and use of EM equipment.

Finally, the subsidence associated with the high pressure air mass behind the front should enhance the layering and the EVD, so the propagation patterns would also look much like before the frontal system influenced the area.

3. Tropical Cyclones

Although a normal threat to the area of study from June to November, tropical cyclones are hardly reflected in the climatological databases. However, their effects clearly affect the EM propagation characteristics in critical operational moments. The tropical cyclone season coincides with higher probability of the occurrence of ducts, enhanced diurnal variability of such occurrences during the summer, and the lowest climatological ASTD.

This study showed smooth profiles in the upper layers and low Z^* values due to increasing winds and mixing ratios. Far from the cyclones' center, a significant superrefractive layer appeared due to the dry air subsidence associated with the outer shear line, and thus, creating extended detection ranges in low levels for all the frequency bands.

At the arrival of the storm, the high winds and strong mixing produced very smooth profiles, very similar to standard profiles. As the storm moved away, Z^* values were again high enough to clearly enhance the detection ranges for upper band radars up to more than 100 km in surface, and then back to a profile very similar to that before the storm.

4. Terrain

Significant differences were also found between the radar antenna directed offshore and inland, with important effects such as many narrow lobes over land, creating a cluttered distribution of the signal patterns, which may be especially disturbing to the detecting systems. The validity of such results is an issue outside the scope of this thesis that needs to be more carefully addressed with better data sources.

5. Antenna Heights

The mean EVD heights *(Z*)* observed under the expected conditions in this environment were very similar to the usual antenna heights of many naval radars. Hence, the EVD had a more significant impact. Examining different combinations of frequencies and antenna heights produced contrasting outcomes not always easily predicted.

It is also important to note that the climatological mean EVD top height was about 15m, very similar to the usual antenna heights of shipborne radars. As expected, the strongest effect of ducts was noticed when the antenna height was just below the top of the EVD (*Z**). The radar horizon can effectively be increased with the antenna height, but when they are very similar, roughly half the radiation beams transmitted from the antenna (assumed to have a 0° elevation in all these scenarios) could be running almost parallel along the top of the EVD. Since these values cannot be taken as "hard limits," the final results can be also be hard to predict.

6. IR Propagation

The models used and their sensitivities to the TAWS allowed inputs have been shown to be truly complex detection range outcomes can be often contrary to intuition. The table of sensitivities included in the user's guide of TAWS shows how the main atmospheric variables (like air temperature, humidity, wind speeds) can be extremely important depending on other factors like the solar and lunar ephemeris, heading of the target and position of the sensor. Further, the relationship between those factors will also drastically change based on TOT and the general operational scenario.

C. OPERATIONAL HIGHLIGHTS

Superrefractive ducts are tactically significant, because RF systems may achieve larger ranges than expected, while also having "holes" where no signal will be present.

On the other hand, subrefraction can reduce the radar horizon and significant probability of fade outs (SDF) related. Although such phenomena were assumed not important in Tropical Littoral environments, warm fronts and thermal layering in those environments can exist. Therefore, they must also be analyzed.

Propagation conditions were certainly different over the ocean than those over land because of diurnal heating, turbulence, and water vapor sources. The factors that provided the most useful insights for the analysis already assessed were:

- Water surface temperatures based on the characteristics of oceanic currents, surges, etc.
- Synoptic patterns, such as the presence of high pressure air masses, absence of low pressures associated with convergence.
- Evidence of coastal breezes and diurnal

In the particular case of clouds, satellite imagery was used only as a guidance to find potential layering (strong negative gradients of humidity), but extensive research and significant advances in techniques for satellite derived soundings, data, and winds, can certainly fill the gaps of required weather profiles, and must be widely investigated.

Particularly for MFRs, serious limitations in detecting low flying aircrafts, combined with a false "awareness" of the operators produced by much better performances on surface detection, or greatly enhanced clutter, may suggest increasing the filtering and reducing the sensitivity of the radar to detect small sea skimming targets effectively.

Lower EVDs can make detection of low surface targets very difficult, while radar capabilities for the Search and Rescue (SAR) of small boats and potential victims of the storm may be enhanced. Similarly, Command and Control of the air assets usually employed (such as helicopters and low flying airplanes) may also be disrupted by the surface based ducts, depending on their relative positions and frequencies used.

Thick SBD (such as those after cold front passed) effectively enhance detection ranges in surface levels, but have associated several distinct gaps, "skip zones," without any detection at all in the surface and near the top of the duct. Higher radar frequencies produce a more uniform coverage along the surface, without severe gaps. This is an

important consideration, because the presence of wide zones of strong detection may create a false feeling of confidence in the operators, if they are not aware of the existence of such blind "holes."

Despite the limitations of radiosonde data being available once every 24 hours, the surface data gave proof of the diurnal variability in the thickness of the EVD, with evident increases in the evenings. When the expected *M* gradients are not very strong, the bottom part of the profiles was more "sensitive" to the surface data available, so appending this data was very important to identify the existence of SBDs, which were found to be thick enough to severely degrade almost any device using frequencies above the L Band (1 GHz); hence, the relevancy of better availability and resolution for both surface and upper air data when more reliable results are required.

The issue of data availability is more critical for IR than it was for the radar examples. Many times the missing parameters must be guessed or derived from others. As a consequence, extremely different values would not be rare, and the decision makers must be aware of that. In any event, the examples shown here must be considered only as a general guidance about such effects, and the importance of thoroughly understanding them has been highlighted.

D. LIMITATIONS IN THE STUDY

The TDAs employed have been designed to ingest compatible data effectively (even through automated links), but for this scenario, this proved to be not very realistic. Littoral environments were shown to change radically in the space of a few hours, so the lack of precise and time frequent enough measurements was the most limiting factor, since they could not be considered truly representative of the atmosphere to describe.

Upper air soundings are very important but do not have enough resolution to describe evaporation ducts, so detailed surface data of air temperature, humidity (or water vapor contents), pressure, wind, and sea surface temperature is a major requirement. The radiosonde data available was complemented with surface data from automated weather stations networks and a tidal station, but still several gaps in the databases were found. Additionally, suspicious data had to be discarded, which prevented a more rigorous statistical evaluation.

Data collection platforms are rather heterogeneous and their databases are not necessarily compatible. Most of their data was in raw format, which complicated their integration and employment.

No operational buoy provided METOC data to describe the actual conditions at sea in this area of interest. This seriously limited the possibility of identifying offshore weather patterns such as diurnal breezes, and hourly changes in temperature or humidity. Since this information is an extremely important requirement, it needs to be seriously considered for future research projects.

E. RECOMMENDATIONS AND PROPOSALS FOR FURTHER RESEARCH

This study was originally aimed at providing insights and guidelines to assist operational commanders and mission planners in their decision making processes. The results and conclusions of this study definitely indicate that more research is required to understand such a complex variety of tactical, environmental and technical issues fully. Additional efforts need to be made to assess and predict the variability of the relevant METOC factors accurately for each specific expected scenario.

Both spatial and time resolution of data can be improved by using data from other platforms, such as buoys, surface stations, other ships, and eventually, satellite derived data and the outputs of computer models. The feasibility of complementing data from alternative data sources, and the added value of such data when used with a TDA in an operational environment, needs to be further studied.

In summary, inherent environmental limitations of EW systems, when employed in a tropical littoral scenario, play a very important role. The evaluation of their combined effects is not a simple task to achieve, because the effects of atmospheric anomalies are hard to detect and even harder to measure. Since EW systems will always be subject to those effects, sometimes with opposing results, their performance can be seriously affected if proper corrections are not made for the specific environment where each device is expected to perform.

Failure to do so will result in a degradation of their effectiveness, significantly compromising the great investments made for such systems, and even the success of their mission, which by no means can be afforded in critical scenarios such as those typical of modern littoral warfare.

LIST OF REFERENCES

Accetta, J. S., Shumaker, D. L., *The Infrared and Electro-Optical Systems Handbook*, Vol. 4, Infrared Information Analysis Center, 2001.

Ahrens, Donald, *Meteorology Today: An Introduction to Weather, Climate, and the Environment*, 5th edition, West Publishing Co., 1994.

Asnani, G. C., *Tropical Meteorology*, Vol 2, Indian Institute of Tropical Meteorology, 1993.

Cooper, Alfred W., Course Notes for *PH3204 (Electro-Optical systems and countermeasures)*, Naval Postgraduate School, 2003 (unpublished).

Davidson, Kenneth L., *Assessment of Atmospheric Factors in EM/EO Propagation*, Course Notes, Department of Meteorology, Naval Postgraduate School, Monterey, California, January 2003.

Ellington, Sidney T., *Special Operations in Littoral Warfare*, Master's Thesis, Naval Postgraduate School, Monterey, California, December 1995.

Ferrari, Jair F., *Refractive Conditions of Amazon Environment and Its Effects on Ground and Airborne Radar and ESM Systems*, Master's Thesis, Naval Postgraduate School, Monterey, California, September 2003.

Fujita, T., Tecson, Jaime, *A Kinematic Analysis of Tropical Storm Based on ATS Cloud Motions,* Satellite and Mesometeorology Research Project, University of Chicago, 1974.

GMCA: *The Global Marine Climatic Atlas*, US Navy Fleet Numerical METOC Detachment, Asheville, North Carolina, 2004, http://navy.ncdc.noaa.gov/products/fleet/gmca.html/ (Last accessed: September 2004).

Goksin, Celalettin, *Evaluation of Tactical Decision Aid Programs for Prediction of Field Performance of IR Sensors*, Master's Thesis, Naval Postgraduate School, Monterey, California, December 2000.

Goldhirsh, J., Dockery, G. D., *Measurement Resolution Criteria for Assessment of Coastal Ducting*, IEE Stevenage. vol. 2, no. 407, pp. 317-322. 1995.

Hastentrath, Stefan, *Climate and Circulation of the Tropics*, Reidel Publishing Co., Dordrecht Holland, 1985.

Holst, Gerald C., *Electro-Optical Imaging System Performance*, 3rd edition, SPIE Press, JCD Pubishing, Winter Park, Florida, 2002.

Janssen, Joris, *Naval Fire Control Faces New Threats,* International Defense Review, 01 October 2002, http://www.4janes.com/ (Posted: 17 September, 2002. Last accessed: September 2004).

_____, *Countering Threats with Naval Electro-Optical Systems*, International Defense Review, 01 June, 2003, http://www.4janes.com/ (Posted: 18 December, 2003. Last accessed: September 2004).

Jeffries, R. A. et al., *Tropical Cyclone Forecasters Reference Guide*, Vol. 2 Tropical Climatology, Technical Report No. 236, Monterey Marine Meteorology Division, U.S. Naval Research Laboratory, Monterey, California, 1992.

JNWS, *Safire (AN/AAQ-22)/ SEAFLIR (AN/KAX-1/2)/ Seastar Safire II*, Jane's Naval Weapons Systems, 01 February, 2004, http://www.4janes.com/ (Posted: 25 February, 2004. Last accessed: September 2004.

Joint Chiefs of Staff, *Joint Publication 3-51: Joint Doctrine for Electronic Warfare*, Washington, D.C., April, 2000.

Lake, Charles, *Target Acquisition Weapons Software Version 3.1.2*, ANG Air Combat Command, Weather Readiness Training Center, Camp Blanding, Florida, 2003 (http://www.fljack.ang.af.mil/ (Last accessed: June 2004).

NAVAIR Systems Command, *US Navy Climatic Study of the Caribbean Sea and the Gulf of Mexico*, Vol. I (West Caribbean Sea and Central American Waters), 50-1C-543, September 1985.

NAWCWPNS Naval Air Warfare Center Weapons Division, *Electronic Warfare and Radar Systems Engineering Handbook*, TP 8347, 4th edition, Point Mugu, California, 1993.

Neri, Filippo, *Introduction to Electronic Defense Systems*, Artech House Inc., Norwood, Massachusetts, 1991.

NOAA Forecast Systems Laboratory, *Radiosonde Database Access Online*, http://raob.fsl.noaa.gov/ (Last accessed: September 2004).

NOAA National Hurricane Center, Miami, Florida, FTP server ftp://ftp.nhc.noaa.gov/pub/surface_maps/ (Last accessed: September 2004).

Ortenburger, L. N., Lawson, S. B., and Paterson, B. J., *Radiosonde Data Analysis IV*, Vols. III and IV, GTE Government Systems Corporation, Western Division, Mountain View, California, 1985.

Pagitt, Ron, Brooks, Randall V., *Air Force Weather Systems Training Workbook TAWS 3.2*, USAF Weather Agency Training Division, Offutt AFB, Nebreska (included in TAWS 3.2 CD).

Scott, Joris, Putting Eyes on the Target, Jane's Navy International, 01 February, 2004, http://www.4janes.com/ (Posted: 07 May, 2003. Last accessed: September 2004).

Skolnik, Merrill I., Introduction to Radar Systems, 3rd ed., McGraw Hill, New York, New York, 2001.

Williams, F. R. et al., *Forecasters Handbook for Central America and Adjacent Waters*, TR 89-08, Naval Environmental Prediction Research Facility, Monterey, California, 1989.

Williamson, Samuel J., *Fundamentals of Air Pollution*, Addison-Wesley, 1973.

THIS PAGE INTENTIONALLY LEFT BLANK

INITIAL DISTRIBUTION LIST

1. Defense Technical Information Center
   Ft. Belvoir, Virginia

2. Dudley Knox Library
   Naval Postgraduate School
   Monterey, California

3. Professor K. L. Davidson
   Department of Meteorology
   Naval Postgraduate School
   Monterey, California

4. Professor David C. Jenn
   Department of Electrical and Computer Engineering
   Naval Postgraduate School
   Monterey, California

5. Professor Dan C. Boger
   Department of Information Sciences
   Naval Postgraduate School
   Monterey, California

6. Professor Phillip A. Durkee
   Department of Meteorology
   Naval Postgraduate School
   Monterey, California

7. CAPT. Jeffrey E. Kline
   Department of Operations Research
   Naval Postgraduate School
   Monterey, California